ON THE INADEQUACY OF OPTIMIZING ALIGNMENT AND UNIFORMITY IN CONTRASTIVE LEARNING OF SENTENCE REPRESENTATIONS

Anonymous authors
Paper under double-blind review

ABSTRACT

Contrastive learning is widely used in areas such as visual representation learning (VRL) and sentence representation learning (SRL). Considering the differences between VRL and SRL in terms of negative sample size and evaluation focus, we believe that the solid findings obtained in VRL may not be entirely carried over to SRL. In this work, we consider the suitability of the decoupled form of contrastive loss, i.e., *alignment* and *uniformity*, in SRL. We find a performance gap between sentence representations obtained by jointly optimizing *alignment* and *uniformity* on the STS task and those obtained using contrastive loss. Further, we find that the joint optimization of *alignment* and *uniformity* during training is prone to overfitting, which does not occur on the contrastive loss. Analyzing them based on the variation of the gradient norms, we find that there is a property of "gradient dissipation" in contrastive loss and believe that it is the key to preventing overfitting. We simulate similar "gradient dissipation" of contrastive loss on four optimization objectives of two forms, and achieve the same or even better performance than contrastive loss on the STS tasks, confirming our hypothesis.

The codes and checkpoints will be released for study upon acceptance.

1 INTRODUCTION

Unsupervised contrastive learning Wu et al. (2018) is originated from visual representation learning (VRL) Chen et al. (2020); He et al. (2020); Grill et al. (2020), and has achieved impressive performances therein. Briefly, contrastive learning forces the representation of an input instance (or "anchor") to be similar to that of an augmented view of the same instance (or "postive example") and to differ from that of a different instance (or "negative example"). One plausible justification of this approach is that minimizing the loss of contrastive learning (or "contrastive loss") is shown to be equivalent to simultaneously minimizing an "alignment loss" and a "uniformity loss", where the former dictates the representation similarity between an instance and its positive examples, and the latter forces the representations of all instances to spread uniformly on the unit sphere in the representation space Wang & Isola (2020). Notably this decomposition of the contrastive loss relies on the condition that the number of negative examples participating in the contrastive loss approaches infinity. For VRL, it is arguable that such a condition holds reasonably well since usually a large number (e.g., 65536 He et al. (2020)) of negative examples are used in a batch.

In recent years, contrastive learning has also been adapted to sentence representation learning (SRL), by fine-tuning the representations obtained from a pretrained language model (e.g. BERT Devlin et al. (2018)) Yan et al. (2021); Giorgi et al. (2021); Gao et al. (2021); Zhang et al. (2022b). Such approaches have demonstrated great performances not only for downstream classification tasks, but also for semantic textual similarity (STS) tasks. It is noteworthy that significantly contrasting VRL, which are primarily evaluated using downstream classification tasks Russakovsky et al. (2015); Krizhevsky et al. (2009), or via "extrinsic" protocols Chiu et al. (2016); Faruqui et al. (2016), SRL particularly emphasizes the STS tasks, or "intrinsic" protocols, when evaluating the quality of learned sentence representations Reimers & Gurevych (2019); Li et al. (2020); Yan et al. (2021); Zhang et al. (2022c). This is because the representations obtained from the pretrained language models have already shown strong transfer capability to downstream tasks Devlin et al. (2018); Liu

et al. (2019) while their similarities are rather poorly correlated with the human-rated similarities Reimers & Gurevych (2019); Li et al. (2020).

Following the justification of contrastive learning in VRLWang & Isola (2020), some works Gao et al. (2021); Zhang et al. (2022b) attribute the success of contrastive learning on the STS tasks to a good balance between *alignment* and *uniformity*. Consequently, alignment and uniformity losses are adopted widely as the key metrics for evaluating the goodness of sentence representations learned from contrastive learning Gao et al. (2021); Zhang et al. (2022b;c;a); Klein & Nabi (2022).

Noting that contrastive learning for SRL in fact only uses a rather small number of negative examples (e.g, 63 Gao et al. (2021); Zhang et al. (2022b) or smaller Zhang et al. (2022c)), in this paper, we question whether the "decomposition principle", or jointly optimizing *alignment* and *uniformity*, adequately explains the performance gain in the STS tasks brought by contrastive learning.

After extensive experiments, we find that optimization using *alignment* and *uniformity* losses produces lower performance than that with contrastive loss in the STS tasks. Moreover, this performance degradation is not reflected by the *alignment* and *uniformity* metrics. Interestingly, we also observe the same phenomenon in contrastive learning with another loss function, Decoupled Contrastive Loss (DCL) Yeh et al. (2021), in which the optimization objectives are very similar to *alignment* and *uniformity*. Our further studies also show that training with such decoupled forms of contrastive loss cause severe overfitting, which does not occur in training with the standard contrastive loss. These observations suggest that *alignment* and *uniformity* losses might not serve suitable substitutes for contrastive loss in SRL and that the success of the standard contrastive learning for SRL can not be adequately explained in terms of *alignment* and *uniformity* properties or some delicate balance between the two.

This paper focuses on uncovering other important factors, beyond *alignment* and *uniformity*, that contribute to the success story of contrastive learning in SRL and explain the performance gap between the training scheme using the contrastive loss and those using a decoupled contrastive loss (in terms of *alignment* and *uniformity* or their equivalent). Specifically, we hypothesize that the training dynamics of the standard contrastive learning for SRL plays an essential role in its effectiveness. To that end, we decompose the gradient of the contrastive loss into an *alignment component* and a *uniformity component* and compare the norms of these two components with their counter-parts in training with the decoupled contrastive losses. Interestingly, we observe a distinct "gradient dissipation" phenomenon in training with the standard contrastive loss: the gradient signal quickly drops and vanishes as soon as the negative example is *adequately further* away from the anchor than the positive example, where the adequacy appears to be reflected by a rather moderate threshold. Notably such a phenomenon does not appear in the training schemes using a decoupled contrastive loss, when the negative sample size is small. This observation led us to believe that "gradient dissipation" plays an essential role in standard contrastive learning.

To validate this hypothesis, we construct two new loss functions, both capable of inducing "gradient dissipation" in their training dynamics. We test them experimentally and observe that indeed training with both losses gives comparable or even better performance in the STS tasks than the standard contrastive loss. Interestingly, similar to the contrastive loss, training with these new loss functions also eliminates the alleviates the overfitting problem observed in training using decouple contrastive losses. This confirms that gradient dissipation serves a key role in the success of contrastive learning for SRL and suggests that properly conditioning the training dynamics is more important than optimizing *alignment* and *uniformity* when not too many negative examples are used.

Along our development, we provide insights as to why gradient dissipation is a desirable property. We also provide additional theoretical justifications on the effectiveness of the new loss functions by showing that they are in fact upper bounds of the standard contrastive loss. Due to page limit, some results, derivations and discussions are presented in Appendix.

2 PRELIMINARY

2.1 CONTRASTIVE LEARNING IN SENTENCE REPRESENTATION LEARNING

Let $\mathbb{C}$ be a set of sentences. For each $x_i \in \mathbb{C}$, we use x'_i to denote an augmented view of x_i. With respect to anchor x_i, x'_i is referred to a positive example, and any x_j or x'_j $(j \neq i)$ is referred to as

Method	$\text{BERT}_{\text{base}}$		$\text{BERT}_{\text{large}}$		$\text{RoBERTa}_{\text{base}}$		$\text{RoBERTa}_{\text{large}}$	
	STS.Avg	TR.Avg	STS.Avg	TR.Avg	STS.Avg	TR.Avg	STS.Avg	TR.Avg
Pretrained	56.70	85.34	54.11	85.52	56.57	83.20	53.90	83.76
$\mathcal{L}_{\text{cl}}$	76.04	86.38	76.83	86.14	77.31	85.23	78.52	85.71
$\mathcal{L}_{\text{a\&u}}$	72.62	87.52	74.58	87.77	72.64	85.09	73.02	85.68
$\mathcal{L}_{\text{dcl}}$	71.13	85.18	72.73	87.06	73.18	85.48	72.43	86.05
$\mathcal{L}_{\text{dcl+}}$	75.25	86.95	77.40	87.85	76.33	84.52	75.63	85.57
$\mathcal{L}_{\text{mpt}}$	77.25	87.56	77.35	87.71	76.42	85.10	**78.84**	86.51
$\mathcal{L}_{\text{met}}$	**78.38**	**87.94**	**78.38**	87.94	**77.38**	**85.74**	78.71	86.42
$\mathcal{L}_{\text{mat}}$	77.76	88.65	77.76	**88.65**	76.95	85.64	78.82	**87.06**

Table 1: Performance of the optimization objectives studied in this paper. All results reported are the average value obtained from three runs. STS.Avg represents the average of Spearman correlation on the seven semantic textual similarity datasets. TR.Avg represents the average of accuracy on the seven downstream classification datasets.

a negative example. There is an encoder mapping each x_i and x_i' to their representations h_i and h_i', which are vectors in $\mathbb{R}^d$. Considering the metric invariance, we usually normalize them to obtain $\hat{h}_i$ and $\hat{h}_i'$, which are constrained on the unit hypersphere S^{d-1} centered at the origin. InfoNCE Loss Oord et al. (2018) or "contrastive loss" for anchor x_i is defined by

$$\mathcal{L}_{\text{cl}} = -\log \frac{\exp\left(\hat{h}_i^T \hat{h}_i'/\tau\right)}{\exp\left(\hat{h}_i^T \hat{h}_i'/\tau\right) + \sum_{j,j\neq i}^{N} \exp\left(\hat{h}_i^T \hat{h}_j'\right)/\tau)} \tag{1}$$

where τ is the temperature hyperparameter and N represents the number of negative samples. The quality of sentence representations is shown to insensitive to N Gao et al. (2021), and a small N, such as 63 Gao et al. (2021); Zhang et al. (2022b) or smaller Zhang et al. (2022c) has shown to be the same sufficient as the bigger one.

2.2 The Decouple Version of Contrastive Loss

Alignment and *uniformity* Wang & Isola (2020) decoupled from contrastive loss are shown to be two significant properties. The losses based on the two properties are defined as

$$\mathcal{L}_{\text{a\&u}} = (1-\lambda)\mathcal{L}_{\text{align}} + \lambda\mathcal{L}_{\text{uniform}} \tag{2}$$

$$\mathcal{L}_{\text{align}}(f;\alpha) \triangleq \mathop{\mathbb{E}}_{(\hat{h}_i,\hat{h}_i')\sim p_{\text{pos}}} \left[\|\hat{h}_i - \hat{h}_i'\|_2^{\alpha}\right], \quad \alpha > 0 \tag{3}$$

$$\mathcal{L}_{\text{uniform}}(f;t) \triangleq \log \mathop{\mathbb{E}}_{\substack{\text{i.i.d}\\(\hat{h}_i,\hat{h}_j')\sim p_{\text{data}}}} \left[e^{-t\|\hat{h}_i - \hat{h}_j'\|_2^2}\right], \quad t > 0 \tag{4}$$

where α, t and λ are three hyperparameters. In the meantime, we follow another work Yeh et al. (2021) on decoupled contrastive learning, which removes the positive sample part from the denominator of contrastive loss:

$$\mathcal{L}_{\text{dcl}} = -\log \frac{\exp\left(\hat{h}_i^T \hat{h}_i'/\tau\right)}{\sum_{j,j\neq i}^{N} \exp\left(\hat{h}_i^T h_j'\right)/\tau} = -\hat{h}_i^T \hat{h}_i'/\tau + \log \sum_{j,j\neq i}^{N} \exp\left(\hat{h}_i^T h_j'\right)/\tau \tag{5}$$

Note that the above two decoupled forms of contrastive loss are treated equally in this paper, since the *alignment* part are recognized as equivalent Yeh et al. (2021) and we proved the *uniformity* part of them have the same lower bound [1], which corresponds to the optimization objective of Minimum Energy Problem on the hypersphere Kuijlaars & Saff (1998); Liu et al. (2018).

[1] The proof is provided in Appendix D

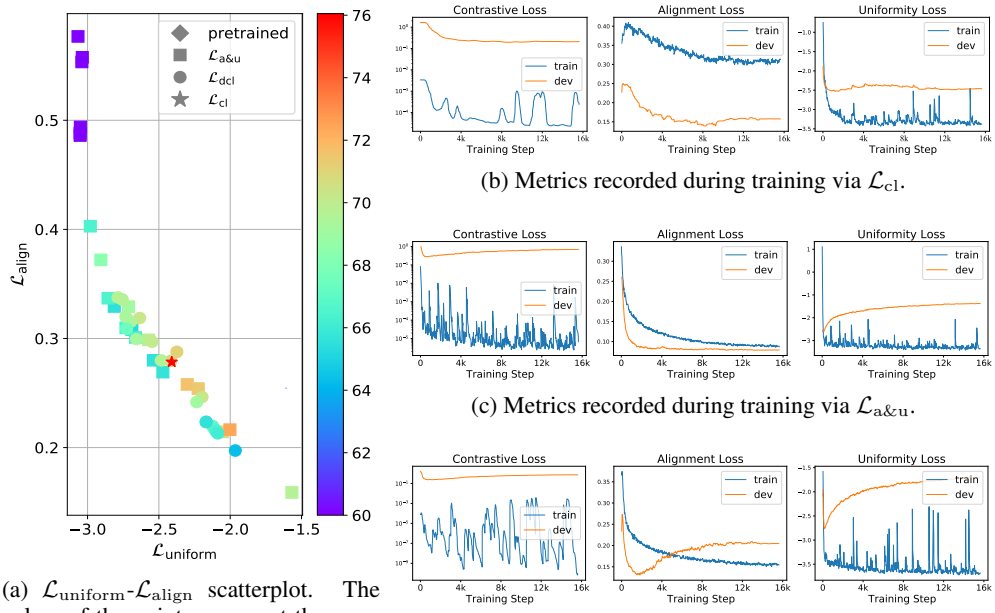

(a) $\mathcal{L}_{\text{uniform}}$-$\mathcal{L}_{\text{align}}$ scatterplot. The colors of the points represent the average Spearman correlation on STS tasks.

(b) Metrics recorded during training via $\mathcal{L}_{\text{cl}}$.

(c) Metrics recorded during training via $\mathcal{L}_{\text{a\&u}}$.

(d) Metrics recorded during training via $\mathcal{L}_{\text{dcl}}$.

Figure 1: The difference between contrastive loss and its two decoupled forms in the training and evaluation phase. All above images are plotted based on the optimization process for $\text{BERT}_{\text{base}}$.

2.3 Performance Comparison

We compare the performance of contrastive loss and its two decoupled forms based on SimCSE Gao et al. (2021), and evaluate with seven datasets on semantic textual similarity (STS) tasks and seven downstream classification datasets on transfer (TR) tasks from the SentEval toolkit Conneau & Kiela (2018). We report the average Spearman correlation for the STS tasks and the average accuracy for the TR tasks in Table 1 . Please refer to Appendix A for experimental details.

As can be seen from the results, we can find that (1) the performance on both STS and TR tasks is better than original pretrained models after optimizing with any one of the three loss functions; (2) the main improvement over the original pretrained models is on the STS tasks, while the improvement on the TR tasks is relatively weak; (3) the decoupled forms obtain the same or better performance on TR tasks as contrastive loss, but there still have a performance gap between them.

These observations reflect to some extent the validity of *alignment* and *uniformity* to replace contrastive loss on TR tasks, but it also implies that there are some other factors playing a key role in the improvement of STS tasks, which have been neglected in the previous studies.

3 The Inadequacy of Optimizing Alignment and Uniformity

3.1 Problem Analysis

To gain a deeper understanding for the above performance gap, we record several metrics during the training and evaluation process, the images of which are shown in Figure 1.

Figure 1a shows the $\mathcal{L}_{\text{uniform}}$-$\mathcal{L}_{\text{align}}$ scatterplot of sentence representations on STS-B Cer et al. (2017) development set, where the colors represent the average Spearman correlation of the STS tasks. It is important to note that the scatterplots of this style are widely used to show that the proposed method is able to achieve a better balance between *alignment* and *uniformity* than other methods Gao et al. (2021); Zhang et al. (2022a;b;c); Klein & Nabi (2022). Indeed, the scatterplot shows that the sentence representations whose ($\mathcal{L}_{\text{uniform}}$, $\mathcal{L}_{\text{align}}$) located in the middle of the image perform better than those whose location in the top left or bottom right. However, the performance

gap between different loss functions are not reflected by the locations in this figure. Specifically, the sentence representations pretrained by $\mathcal{L}_{\text{cl}}$ and its decoupled forms have the almost same *alignment* and *uniformity*, but different performance on the STS tasks.

Figure 1b shows the numerical variation of $\mathcal{L}_{\text{cl}}$, $\mathcal{L}_{\text{align}}$ and $\mathcal{L}_{\text{uniform}}$ on the training set and development set during the optimization process with $\mathcal{L}_{\text{cl}}$. In terms of trends, all metrics on both the training set and development set first decrease and then remain flat, which can be seen as a reference for normal training in the study.

Figure 1c and 1d show the same metrics during the optimization process with $\mathcal{L}_{\text{a\&u}}$ and $\mathcal{L}_{\text{dcl}}$. Comparing with Figure 1b, the variation trends of the two figures show different degrees of overfitting. Specifically, when $\mathcal{L}_{\text{a\&u}}$ is applied for optimization, all metrics except $\mathcal{L}_{\text{align}}$ show first decrease and then increase in the development set, while the similar situation occurs in all three metrics when $\mathcal{L}_{\text{dcl}}$ is applied.

3.2 Optimization Dynamics Study

Since $\mathcal{L}_{\text{a\&u}}$ and $\mathcal{L}_{\text{dcl}}$ can be treated as equivalent to $\mathcal{L}_{\text{cl}}$ only when negative samples tend to infinity, we need to pay attention to what exactly is the difference between them when the number of negative samples is small. To gain more insights on their differences, we investigate the gradient property between contrastive loss and its decoupled forms in optimization dynamics. [2]

The gradient of $\mathcal{L}_{\text{cl}}$ for the anchor h_i can be split into $\nabla_{\text{cl}}^{\text{pos}}$ and $\nabla_{\text{cl}}^{\text{neg}}$:

$$\frac{\partial \mathcal{L}_{\text{cl}}}{\partial h_i} = \underbrace{-\frac{1}{\tau}\frac{\sum_{j,j\neq i}^{N}\exp\left(\hat{h}_i^T\hat{h}_j'/\tau\right)\left(\hat{h}_i'-\hat{h}_i\right)}{\exp\left(\hat{h}_i^T\hat{h}_i'/\tau\right)+\sum_{j,j\neq i}^{N}\exp\left(\hat{h}_i^T\hat{h}_j'/\tau\right)}\frac{I-M_{h_i}}{\|h_i\|}}_{\nabla_{\text{cl}}^{\text{pos}}} + \underbrace{\frac{1}{\tau}\frac{\sum_{j,j\neq i}^{N}\exp\left(\hat{h}_i^T\hat{h}_j'/\tau\right)\left(\hat{h}_j'-\hat{h}_i\right)}{\exp\left(\hat{h}_i^T\hat{h}_i'/\tau\right)+\sum_{j,j\neq i}^{N}\exp\left(\hat{h}_i^T\hat{h}_j'/\tau\right)}\frac{I-M_{h_i}}{\|h_i\|}}_{\sum_{j,j\neq i}^{N}\nabla_{\text{cl}}^{\text{neg}_j}} \tag{6}$$

where I is the identity matrix and M_{h_i} is the projection matrix on h_i. The first term $\nabla_{\text{cl}}^{\text{pos}}$ points from $\hat{h}_i$ to $\hat{h}_i'$, "pulling" the anchor and the positive sample close to optimize *alignment*, while the second term $\nabla_{\text{cl}}^{\text{neg}}$ points from $\hat{h}_i$ to $\hat{h}_j'$, pushing the anchor away from the negative samples to optimize *uniformity*. Then the gradient norm on *alignment* is computed:

$$\left\|\nabla_{\text{cl}}^{\text{pos}}\right\| = \frac{1}{\tau}\frac{\sum_{j,j\neq i}^{N}\exp\left(\cos\theta_{ij'}/\tau\right)\left\|\hat{h}_i'-\cos\theta_{ii'}\hat{h}_i\right\|}{\exp\left(\cos\theta_{ii'}/\tau\right)+\sum_{j,j\neq i}^{N}\exp\left(\cos\theta_{ij'}/\tau\right)}\frac{1}{\|h_i\|} = \frac{1}{\tau}\frac{\sum_{j,j\neq i}^{N}\exp\left(\cos\theta_{ij'}/\tau\right)\sin\theta_{ii'}}{\exp\left(\cos\theta_{ii'}/\tau\right)+\sum_{j,j\neq i}^{N}\exp\left(\cos\theta_{ij'}/\tau\right)}\frac{1}{\|h_i\|} \tag{7}$$

where $\theta_{ii'}$ represents the angle between the anchor $\hat{h}_i$ and the positive sample $\hat{h}_i'$, and $\theta_{ij'}$ represents the angle between the anchor $\hat{h}_i$ and the negative sample $\hat{h}_j'$. Likewise, we give the gradient norm of $\mathcal{L}_{\text{align}}$ and $\mathcal{L}_{\text{dcl}}$ on *alignment*:

$$\left\|\frac{\partial \mathcal{L}_{\text{align}}}{\partial h_i}\right\| = \|\nabla\mathcal{L}_{\text{align}}\| = \frac{\alpha(2\sin\left(\theta_{ii'}/2\right))^{\alpha-2}}{\|h_i\|}\left\|\hat{h}_i'-\cos\theta_{ii'}\hat{h}_i\right\| = \frac{\alpha(2\sin\left(\theta_{ii'}/2\right))^{\alpha-2}sin\theta_{ii'}}{\|h_i\|} \tag{8}$$

$$\|\nabla_{\text{dcl}}^{\text{pos}}\| = \frac{1}{\tau\|h_i\|}\left\|\hat{h}_i'-\cos\theta_{ii'}\hat{h}_i\right\| = \frac{\sin\theta_{ii'}}{\tau\|h_i\|} \tag{9}$$

Comparing equation 7, 8 and 9, we find that the gradient directions of these three parts are the same, but a key difference among them is that $\theta_{ij'}$ is contained in $\|\nabla_{\text{cl}}^{\text{pos}}\|$ but not in $\|\nabla\mathcal{L}_{\text{align}}\|$ neither in $\|\nabla_{\text{dcl}}^{\text{pos}}\|$, which will cause the gradient signal on *alignment* to be independent of $\theta_{ij'}$.

Figure 2a visualize this difference by plotting the heatmaps of $\|\nabla_{\text{cl}}^{\text{pos}}\|$, $\|\nabla\mathcal{L}_{\text{align}}\|$ and $\|\nabla_{\text{dcl}}^{\text{pos}}\|$ with $\theta_{ii'}$-$\theta_{ij'}$. The leftmost four plots show the $\|\nabla_{\text{cl}}^{\text{pos}}\|$ under the different number of negative samples, while the rightmost two plots show $\|\nabla\mathcal{L}_{\text{align}}\|$ and $\|\nabla_{\text{dcl}}^{\text{pos}}\|$ under the condition of 64 negative sample size. Observing the leftmost four plots, we can find that the area of the shaded part (or the area with weak gradient signals) gradually decreases as the number of negative samples increases. Therefore, it is conceivable that when the number of negative samples tends to infinity, these images will gradually become identical to the two rightmost images.

[2] Please refer to the Appendix C for the derivation of all formulas in this section and the subsequent ones. Due to the space limitation of the main text, only the gradients related to the *alignment* part are analyzed here, please refer to Appendix B for the analysis of the *uniformity* part.

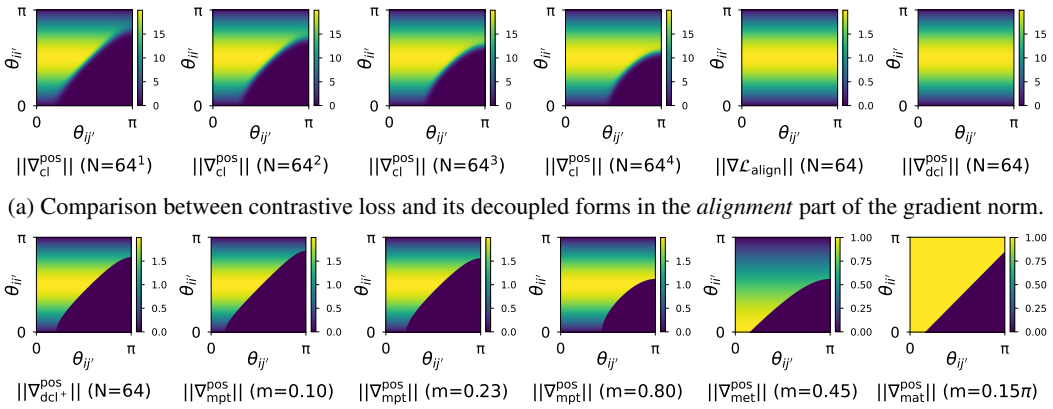

(a) Comparison between contrastive loss and its decoupled forms in the *alignment* part of the gradient norm.

(b) Comparison among the proposed loss functions for validation in the *alignment* part of the gradient norm.

Figure 2: Gradient norms of all the loss functions studied in the main text with respect to the *alignment* part. When the images are plotted, the $1/\|h_i\|$ in equations are ignored; all $\theta_{ij'}$ in one equation are treated as the same value; all hyperparameters in equations are consistent with the columns corresponding to $\text{BERT}_{\text{base}}$ in Table 2.

Comparing the leftmost plot with the rightmost two plots, we can clearly see the difference between them, where the former has a "gradient dissipation" situation that the latter does not have. So let us think what will happen during training. $\theta_{ij'}$ will increase and $\theta_{ii'}$ will decrease gradually. For $\|\nabla_{\text{cl}}^{\text{pos}}\|$, the gradient signs of some anchors will suddenly dissipate at a certain time and only the anchors whose $\theta_{ij'}$ is not too larger than $\theta_{ii'}$ will still receive the gradient signals. For $\|\nabla\mathcal{L}_{\text{align}}\|$ and $\|\nabla_{\text{dcl}}^{\text{pos}}\|$, since they are not constrained by $\theta_{ij'}$, their gradient signals will do not vary with the horizontal axis. All anchors except those with absolutely small $\theta_{ii'}$ will receive a continuous gradient signal during the training process.

We point out that the above qualitative conclusion does not fail to hold if the angle is replaced with a generic distance function $\rho(.,.)$ on the hypersphere. Therefore, the difference on "gradient dissipation" can be intuitively described as: "When the number of negative samples is small, contrastive loss tries to keep $\rho(\hat{h_i}, \hat{h'_i})$ small relative to $\rho(\hat{h_i}, \hat{h'_j})$ by some value, while its decoupled forms try to keep $\theta_{ii'}$ absolutely small". Here, we unthinkingly hypothesize that the "gradient dissipation" is a key property in the performance gap between contrastive loss and its decoupled form, and more insights on this hypothesis will be provided in Section 5.

4 Experimental verification

4.1 Validation via the introduction of $\mathcal{L}_{\text{dcl}^+}$

To validate our hypothesis, we try to simulate this property with the smallest possible changes. Then we notice two facts: (1) $\mathcal{L}_{\text{dcl}}$ will gradually become negative as training proceeds; (2) the "gradient dissipation" only occurs when $\theta_{ij'}$ is large enough with respect to $\theta_{ii'}$. These two facts inspire us to introduce a ReLU function Glorot et al. (2011) on top of $\mathcal{L}_{\text{dcl}}$ to force the truncation of the gradient signal of the anchor when $\mathcal{L}_{\text{dcl}} < 0$:

$$\mathcal{L}_{\text{dcl}^+} = max\left(-\hat{h}_i^T\hat{h}'_i/\tau + \log\left(\sum_{j,j\neq i}^{N}\exp\left(\hat{h}_i^T\hat{h}'_j\right)/\tau\right), 0\right) \tag{10}$$

Likewise, we can obtain its gradient norm associated with *alignment*:

$$\left\|\nabla_{\text{dcl}^+}^{\text{pos}}\right\| = \begin{cases} \dfrac{\sin\theta_{ij'}}{\tau}\dfrac{1}{\|h_i\|}, & -\hat{h}_i^T\hat{h}'_i/\tau + \log\sum_{j,j\neq i}^{N}\exp\left(\hat{h}_i^T\hat{h}'_j\right)/\tau > 0 \\ 0, & -\hat{h}_i^T\hat{h}'_i/\tau + \log\sum_{j,j\neq i}^{N}\exp\left(\hat{h}_i^T\hat{h}'_j\right)/\tau \leq 0 \end{cases} \tag{11}$$

The leftmost plot of Figure 2b shows $\left\|\nabla_{\text{dcl}^+}^{\text{pos}}\right\|$ under the condition of 64 negative sample size. Comparing with the leftmost plot of Figure 2a, we can the images of $\left\|\nabla_{\text{dcl}^+}^{\text{pos}}\right\|$ and $\|\nabla_{\text{cl}}^{\text{pos}}\|$ are almost

identical, which proves that the added ReLU function can indeed simulate the property of "gradient dissipation". More importantly, the experimental results in Table 1 demonstrate the effectiveness of $\mathcal{L}_{\text{dcl+}}$, which boosts 3%-7% on the STS tasks in the different pretrained models.

4.2 VALIDATION VIA THE UPPER BOUNDS FOR $\mathcal{L}_{\text{cl}}$

In fact, $\mathcal{L}_{\text{dcl+}}$ is introduced not only for the above mentioned observations, but also because it can be proved to be the upper bound of $\mathcal{L}_{\text{cl}}$. Further, we find that another upper bound with the property of "gradient dissipation", which can be derived after a second relaxation based on $\mathcal{L}_{\text{dcl+}}$:

$$\begin{aligned}\mathcal{L}_{\text{cl}} &\leq \log 2 + \max\left(-\hat{h}_i^T \hat{h}_i'/\tau + \log \textstyle\sum_{j,j\neq i}^{N} \exp\left(\hat{h}_i^T \hat{h}_j'/\tau\right), 0\right) = \log 2 + \mathcal{L}_{\text{dcl+}} \\ &\leq \log 2 + \frac{1}{\tau} \max\left(-\hat{h}_i^T \hat{h}_i' + \max_{i,j\neq i}\left(\hat{h}_i^T \hat{h}_j\right) + \tau \log(N-1), 0\right)\end{aligned} \tag{12}$$

where $\tau \log(N-1)$ can be replace as the margin hyperparameter m. Then we can get a new loss function:

$$\mathcal{L}_{\text{mpt}} = \max\left(-\hat{h}_i^T \hat{h}_i' + \max_{j,j\neq i} \hat{h}_i^T \hat{h}_j + m, 0\right) \tag{13}$$

Note that the new upper bound is very close in form to Tripet Loss Weinberger & Saul (2009), but the most hard negative sample is selected for optimization in this form, so we call the loss function $\mathcal{L}_{\text{mpt}}$ (Minimum dot Product Triplet Loss).

To increase the variation diversity of gradient norm, we replace the dot product with the Euclidean distance to obtain $\mathcal{L}_{\text{met}}$ (Minimum Euclidean distance Triplet Loss) and the angle to obtain $\mathcal{L}_{\text{mat}}$ (Minimum Angle Triplet Loss):

$$\mathcal{L}_{\text{met}} = \max\{\|\hat{h}_i - \hat{h}_i'\|_2 - \min_{j,j\neq i} \|\hat{h}_i - \hat{h}_j'\|_2 + m, 0\} \tag{14}$$

$$\mathcal{L}_{\text{mat}} = \max\{\theta_{ii'} - \min_{j,j\neq i} \theta_{ij'} + m, 0\} \tag{15}$$

We also report their results in Table 1. We find that the performance of these loss functions ahead of the decoupled forms of contrastive loss, and is comparable to or better than contrastive loss. Likewise, their gradient norm associated with *alignment*, $\left\|\nabla_{mpt}^{pos}\right\|$, $\|\nabla_{\text{met}}^{\text{pos}}\|$ and $\|\nabla_{\text{mat}}^{\text{pos}}\|$, are plotted in Figure 4c. There are some difference among these gradient norms due to the choice of different distance functions, but it does not bring about a significant difference in their performance. Therefore, the effectiveness of the "gradient dissipation" property is further affirmed by controlling variables.

4.3 MECHANISTIC ANALYSIS OF GRADIENT DISSIPATION

We develop a interest in $\mathcal{L}_{\text{mpt}}$ because the degree of "gradient dissipation" can be adjusted by the parameter m (Figure 2b) and independent of the number of negative samples. Therefore, we can quantitatively observe how the value of margin effect the performance with this more flexible form.

Recalling that the "gradient dissipation" occurs when $d_{ij} = \|\rho(\hat{h}_i, \hat{h}_j') - \rho(\hat{h}_i, \hat{h}_i')\|$ is outside a certain range, in $\mathcal{L}_{mpt}$, where $\rho(.,.)$ is a distance function. Therefore, we can obtain different mean value of d_{ij} by selecting different m during training. Figure 3a shows that how the performance on STS tasks and TR tasks varies with d_{ij}. Then we can find that the performance of STS tasks are much more sensitive to d_{ij} than the TR task's, and too large or too small a d_{ij} will cause the performance of the STS task to drop sharply. In contrast, the performance of the TR task does not vary significantly with d_{ij}, which seems to explain to some extent why the decoupled form can work well in VRL. What's more, it can be seen that a suitable margin value helps to achieve a double-best performance for both STS and TR tasks, which indicates that sentence representation quality can achieve some sense of synthetic optimality and that there is no significant mutual exclusivity between intrinsically and extrinsically evaluated performance.

To better understand the first observation, we set m to 0.10, 0.23 (corresponding the best performance) and 0.80 respectively, and record the numerical variation of $\mathcal{L}_{\text{cl}}$, $\mathcal{L}_{\text{align}}$ and $\mathcal{L}_{\text{uniform}}$ on the training and development sets. Comparing Figure 3c and 3d first, which reflect the cases when m is 0.10 and 0.23. We find that $\mathcal{L}_{\text{cl}}$ can drop to lower on both training and validation sets when m is 0.23, and this difference is magnified by the $\mathcal{L}_{\text{uniform}}$, while $\mathcal{L}_{\text{align}}$ remains almost constant. It is consistent with our intuition, when m is too small, the gradient signal may be weak at the beginning

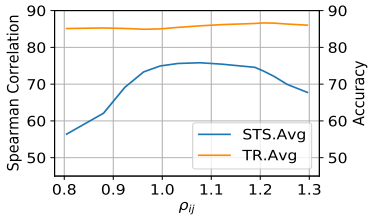

(a) Effects of ρ_{ij} on performance.

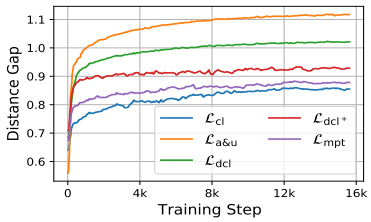

(b) The average gap between $\rho(\hat{h}_i, \hat{h}'_j)$ and $\rho(\hat{h}_i, \hat{h}'_i)$ during training when the different loss functions are adopted for optimization.

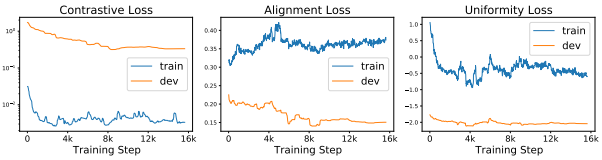

(c) Metrics recorded during training via $\mathcal{L}_{\text{mpt}}(m = 0.10)$.

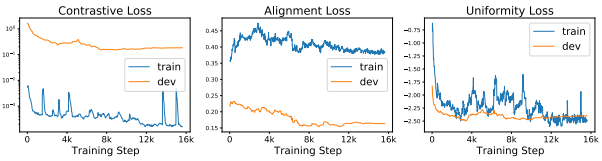

(d) Metrics recorded during training via $\mathcal{L}_{\text{mpt}}(m = 0.23)$.

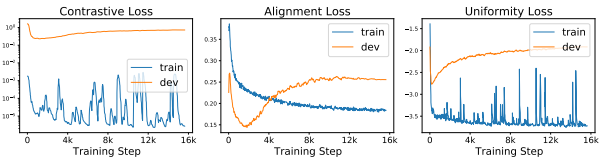

(e) Metrics recorded during training via $\mathcal{L}_{\text{mpt}}(m = 0.80)$.

Figure 3: The plots of the loss functions proposed in this work. In Figure (b), $\rho(.,.)$ presents Euclidean distance. We first calculate the average distance of all negative samples to the anchor, then subtract the distance of positive samples to anchor from it to get the distance gap, and finally plot the average distance gap of all anchor in the mini-batch in the figure. All above images are plotted based on the optimization process for $\text{BERT}_{\text{base}}$.

of the optimization, leading to no improvement in the uniformity of the representation vectors. Then turn our attention to Figure 3e, which plots the same metrics when m is 0.80. The curves as a whole is highly similar to Figure 1d, with the same overfitting phenomenon. It is also intuitive, since an excessively large margin leads the optimization process exceptionally difficult, thus preventing the "gradient dissipation" phenomenon from occurring during the optimization process. To summarize, the above phenomenon further illustrates that the timing of gradient dissipation is very important; too early "gradient dissipation" will result in under-tuned models, while too late "gradient dissipation" will result in degraded model performance and overfitting of training. Further, in Appendix E, we study the relation between $\mathcal{L}_{\text{mpt}}$ and the Mixup-based approaches Kalantidis et al. (2020); Zhang et al. (2022b).

5 Discussion

In this section, we share some thoughts and observations to explain why we believe that the "gradient dissipation" plays a key role in SRL. We start by considering it in the relation to the STS tasks. For consistency with the retrieval scenario in practice, the STS tasks care about the relative order among sentence distances rather than the absolute value Reimers & Gurevych (2019). Therefore, in the ideal case, we should let the samples closer to the anchor if they are more semantically similar to the anchor, and does not need to care about the absolute distance to the anchor. Intuitively, the property of "gradient dissipation" only works to puts negative samples further away from the anchor compared to positive samples, which is consistent with the need for STS tasks.

On the other hand, *alignment* and *uniformity* only describe the relation between the anchor and its samples, while ignoring the relations between the positive samples and the negative samples. In other words, this optimization form overemphasizes the characteristics of the individual sentence itself and ignores the actual connections between the semantics. In early exploratory trials, we find that the distance gap between negative sample-anchor and positive sample points is continuously enlarged when the decouple forms are adopted for optimization (Figure 3b), which is far beyond

the level when optimized by contrastive loss. Considering the limitations of data augmentation to generate positive samples and the noise in negative samples, we suspect that it compromises the original semantic information of the pretrained models to some extent.

Combining on the above thoughts and observations, we hypothesize that the "gradient dissipation" property is responsible for the better performance in the STS evaluation.

6 Related Work

Sentence representation learning (SRL) Kiros et al. (2015); Conneau et al. (2017); Reimers & Gurevych (2019); Li et al. (2020) is one of the fundamental tasks in NLP, aiming at learning semantically rich high-dimensional representation at the sentence level. The good sentence representations need to satisfy both (1) high correlation with human-rated similarities (intrinsic evaluation) and (2) good transferability (extrinsic evaluation) Chiu et al. (2016); Faruqui et al. (2016).

The pretrained language models Peters et al. (2018); Devlin et al. (2018); Liu et al. (2019) were once regraded as the source for obtaining universal sentence representations, and the sentence representations obtained by pretrained models have shown extraordinary performance on tranfer tasks. However, these sentence representations obtained from the pretrained models even get lower performance than the average Glove embeddings Pennington et al. (2014) on semantic textual similarity (STS) tasks Reimers & Gurevych (2019). Then more studies have found the word representation space of pretrained models, such as BERT Devlin et al. (2018) and ELMo Peters et al. (2018), are anisotropic Ethayarajh (2019), where word embeddings are concentrated on a high-dimensional conical space Gao et al. (2018).

Early works Li et al. (2020); Su et al. (2021) try to diminish the anisotropy of the pretrained representation space using the whitening transformation Su et al. (2021) or the flow function Li et al. (2020). These approaches are easy to implement, but limited improvement for STS tasks. Recently, contrastive learning methods based on instance discrimination Zhang et al. (2022b;c;a) are introduced to SRL. However, a great deal of works Yan et al. (2021); Gao et al. (2021); Zhou et al. (2022); Zhang et al. (2022b) focus on how to obtain or generate better positive and negative samples. At the same time, we find that even though there are significant differences in current contrastive learning methods in VRL and SRL, such as differences in pretraining and fine tuning, and differences in negative sample sizes (see Section 1 for details), few works have dabbled in the optimization mechanisms of contrastive learning in SRL. Instead, a large number of findings from VRL, such as *alignment* and *uniformity* Wang & Isola (2020); Gao et al. (2021), momentum updates He et al. (2020); Wu et al. (2021) and bootstrap Grill et al. (2020); Cao et al. (2022), have been directly applied.

Although there are a large number of works Gao et al. (2021); Zhang et al. (2022b;c;a); Klein & Nabi (2022) in SRL that use *alignment* and *uniformity* as evaluation metrics, to our knowledge, this work first study their inadequacy as the optimization objectives in SRL.

7 Conclusion

In this paper, we focus on the performance gap between contrastive loss and its decoupled forms, i.e., *alignment* and *uniformity* in SRL. Our series of new findings contribute to a deeper understanding of how contrastive loss can improve the quality of sentence representation on STS tasks: (1) *Alignment* and *Uniformity* Loss or their equivalent are not suitable as alternative loss functions for contrastive loss in SRL due to their lower performance and overfitting problem; (2) The "gradient dissipation" property of contrastive loss under a small number of negative samples plays a key role in the performance on STS tasks and preventing overfitting; (3) The "gradient dissipation" property works to control a suitable distance gap of anchor-positive and anchor-negative samples, while *alignment* and *uniformity* are the properties that control the absolute distance of them; (4) Other two loss functions with "gradient dissipation" property also can solve the overfitting problem, and obtain the same or even better performance than contrastive loss, even if their "gradient dissipation" properties are not sensitive to the number of negative samples.

We hope these findings to build a better understanding to the key properties of contrastive loss in SRL. Further, some new loss functions that are not bound to the form of contrastive loss can be designed via these properties, improving the quality of the sentence representation synthetically.

REFERENCES

Eneko Agirre, Daniel Cer, Mona Diab, and Aitor Gonzalez-Agirre. Semeval-2012 task 6: A pilot on semantic textual similarity. In ** SEM 2012: The First Joint Conference on Lexical and Computational Semantics–Volume 1: Proceedings of the main conference and the shared task, and Volume 2: Proceedings of the Sixth International Workshop on Semantic Evaluation (SemEval 2012)*, pp. 385–393, 2012.

Eneko Agirre, Daniel Cer, Mona Diab, Aitor Gonzalez-Agirre, and Weiwei Guo. * sem 2013 shared task: Semantic textual similarity. In *Second joint conference on lexical and computational semantics (* SEM), volume 1: proceedings of the Main conference and the shared task: semantic textual similarity*, pp. 32–43, 2013.

Eneko Agirre, Carmen Banea, Claire Cardie, Daniel Cer, Mona Diab, Aitor González-Agirre, Weiwei Guo, Rada Mihalcea, German Rigau, and Janyce Wiebe. Semeval-2014 task 10: Multilingual semantic textual similarity. In *Proceedings of the 8th International Workshop on Semantic Evaluation (SemEval 2014)*, pp. 81–91, 2014.

Eneko Agirre, Carmen Banea, Claire Cardie, Daniel Cer, Mona Diab, Aitor Gonzalez-Agirre, Weiwei Guo, Inigo Lopez-Gazpio, Montse Maritxalar, Rada Mihalcea, et al. Semeval-2015 task 2: Semantic textual similarity, english, spanish and pilot on interpretability. In *Proceedings of the 9th international workshop on semantic evaluation (SemEval 2015)*, pp. 252–263, 2015.

Eneko Agirre, Carmen Banea, Daniel Cer, Mona Diab, Aitor González-Agirre, Rada Mihalcea, German Rigau, and Janyce Wiebe. Semeval-2016 task 1: Semantic textual similarity, monolingual and cross-lingual evaluation. In *Proceedings of the 10th International Workshop on Semantic Evaluation (SemEval-2016)*, pp. 497–511, 2016.

Rui Cao, Yihao Wang, Yuxin Liang, Ling Gao, Jie Zheng, Jie Ren, and Zheng Wang. Exploring the impact of negative samples of contrastive learning: A case study of sentence embedding. In *Findings of the Association for Computational Linguistics: ACL 2022*, pp. 3138–3152, 2022.

Daniel Cer, Mona Diab, Eneko Agirre, Iñigo Lopez-Gazpio, and Lucia Specia. Semeval-2017 task 1: Semantic textual similarity multilingual and crosslingual focused evaluation. In *Proceedings of the 11th International Workshop on Semantic Evaluation (SemEval-2017)*, pp. 1–14, 2017.

Ting Chen, Simon Kornblith, Mohammad Norouzi, and Geoffrey Hinton. A simple framework for contrastive learning of visual representations. In *International conference on machine learning*, pp. 1597–1607. PMLR, 2020.

Billy Chiu, Anna Korhonen, and Sampo Pyysalo. Intrinsic evaluation of word vectors fails to predict extrinsic performance. In *Proceedings of the 1st workshop on evaluating vector-space representations for NLP*, pp. 1–6, 2016.

Alexis Conneau and Douwe Kiela. Senteval: An evaluation toolkit for universal sentence representations. *arXiv preprint arXiv:1803.05449*, 2018.

Alexis Conneau, Douwe Kiela, Holger Schwenk, Loïc Barrault, and Antoine Bordes. Supervised learning of universal sentence representations from natural language inference data. In *Proceedings of the 2017 Conference on Empirical Methods in Natural Language Processing*, pp. 670–680, 2017.

Jacob Devlin, Ming-Wei Chang, Kenton Lee, and Kristina Toutanova. Bert: Pre-training of deep bidirectional transformers for language understanding. *arXiv preprint arXiv:1810.04805*, 2018.

William B Dolan and Chris Brockett. Automatically constructing a corpus of sentential paraphrases. In *Proceedings of the Third International Workshop on Paraphrasing (IWP2005)*, 2005.

Kawin Ethayarajh. How contextual are contextualized word representations? comparing the geometry of bert, elmo, and gpt-2 embeddings. In *Proceedings of the 2019 Conference on Empirical Methods in Natural Language Processing and the 9th International Joint Conference on Natural Language Processing (EMNLP-IJCNLP)*, pp. 55–65, 2019.

Manaal Faruqui, Yulia Tsvetkov, Pushpendre Rastogi, and Chris Dyer. Problems with evaluation of word embeddings using word similarity tasks. *ACL 2016*, pp. 30, 2016.

Jun Gao, Di He, Xu Tan, Tao Qin, Liwei Wang, and Tieyan Liu. Representation degeneration problem in training natural language generation models. In *International Conference on Learning Representations*, 2018.

Tianyu Gao, Xingcheng Yao, and Danqi Chen. Simcse: Simple contrastive learning of sentence embeddings. In *EMNLP*, 2021.

John Giorgi, Osvald Nitski, Bo Wang, and Gary Bader. Declutr: Deep contrastive learning for unsupervised textual representations. In *Proceedings of the 59th Annual Meeting of the Association for Computational Linguistics and the 11th International Joint Conference on Natural Language Processing (Volume 1: Long Papers)*, pp. 879–895, 2021.

Xavier Glorot, Antoine Bordes, and Yoshua Bengio. Deep sparse rectifier neural networks. In *Proceedings of the fourteenth international conference on artificial intelligence and statistics*, pp. 315–323. JMLR Workshop and Conference Proceedings, 2011.

Jean-Bastien Grill, Florian Strub, Florent Altché, Corentin Tallec, Pierre Richemond, Elena Buchatskaya, Carl Doersch, Bernardo Avila Pires, Zhaohan Guo, Mohammad Gheshlaghi Azar, et al. Bootstrap your own latent-a new approach to self-supervised learning. *Advances in neural information processing systems*, 33:21271–21284, 2020.

Kaiming He, Haoqi Fan, Yuxin Wu, Saining Xie, and Ross Girshick. Momentum contrast for unsupervised visual representation learning. In *2020 IEEE/CVF Conference on Computer Vision and Pattern Recognition (CVPR)*, pp. 9726–9735. IEEE Computer Society, 2020.

Minqing Hu and Bing Liu. Mining and summarizing customer reviews. In *Proceedings of the tenth ACM SIGKDD international conference on Knowledge discovery and data mining*, pp. 168–177, 2004.

Yannis Kalantidis, Mert Bulent Sariyildiz, Noe Pion, Philippe Weinzaepfel, and Diane Larlus. Hard negative mixing for contrastive learning. *Advances in Neural Information Processing Systems*, 33:21798–21809, 2020.

Ryan Kiros, Yukun Zhu, Russ R Salakhutdinov, Richard Zemel, Raquel Urtasun, Antonio Torralba, and Sanja Fidler. Skip-thought vectors. *Advances in neural information processing systems*, 28, 2015.

Tassilo Klein and Moin Nabi. SCD: Self-contrastive decorrelation of sentence embeddings. In *Proceedings of the 60th Annual Meeting of the Association for Computational Linguistics (Volume 2: Short Papers)*, pp. 394–400, Dublin, Ireland, May 2022. Association for Computational Linguistics. doi: 10.18653/v1/2022.acl-short.44. URL `https://aclanthology.org/2022.acl-short.44`.

Alex Krizhevsky et al. Learning multiple layers of features from tiny images. 2009.

Arno Kuijlaars and E Saff. Asymptotics for minimal discrete energy on the sphere. *Transactions of the American Mathematical Society*, 350(2):523–538, 1998.

Bohan Li, Hao Zhou, Junxian He, Mingxuan Wang, Yiming Yang, and Lei Li. On the sentence embeddings from pre-trained language models. In *Proceedings of the 2020 Conference on Empirical Methods in Natural Language Processing (EMNLP)*, pp. 9119–9130, 2020.

Weiyang Liu, Rongmei Lin, Zhen Liu, Lixin Liu, Zhiding Yu, Bo Dai, and Le Song. Learning towards minimum hyperspherical energy. *Advances in neural information processing systems*, 31, 2018.

Yinhan Liu, Myle Ott, Naman Goyal, Jingfei Du, Mandar Joshi, Danqi Chen, Omer Levy, Mike Lewis, Luke Zettlemoyer, and Veselin Stoyanov. Roberta: A robustly optimized bert pretraining approach. *arXiv preprint arXiv:1907.11692*, 2019.

Marco Marelli, Stefano Menini, Marco Baroni, Luisa Bentivogli, Raffaella Bernardi, and Roberto Zamparelli. A sick cure for the evaluation of compositional distributional semantic models. In *Proceedings of the Ninth International Conference on Language Resources and Evaluation (LREC'14)*, pp. 216–223, 2014.

Aaron van den Oord, Yazhe Li, and Oriol Vinyals. Representation learning with contrastive predictive coding. *arXiv preprint arXiv:1807.03748*, 2018.

Bo Pang and Lillian Lee. A sentimental education: Sentiment analysis using subjectivity summarization based on minimum cuts. In *Proceedings of the 42nd Annual Meeting of the Association for Computational Linguistics (ACL-04)*, pp. 271–278, 2004.

Bo Pang and Lillian Lee. Seeing stars: Exploiting class relationships for sentiment categorization with respect to rating scales. In *Proceedings of the 43rd Annual Meeting of the Association for Computational Linguistics (ACL'05)*, pp. 115–124, 2005.

Jeffrey Pennington, Richard Socher, and Christopher D Manning. Glove: Global vectors for word representation. In *Proceedings of the 2014 conference on empirical methods in natural language processing (EMNLP)*, pp. 1532–1543, 2014.

Matthew E. Peters, Mark Neumann, Mohit Iyyer, Matt Gardner, Christopher Clark, Kenton Lee, and Luke Zettlemoyer. Deep contextualized word representations. In *Proceedings of the 2018 Conference of the North American Chapter of the Association for Computational Linguistics: Human Language Technologies, Volume 1 (Long Papers)*, pp. 2227–2237, New Orleans, Louisiana, June 2018. Association for Computational Linguistics. doi: 10.18653/v1/N18-1202. URL https://aclanthology.org/N18-1202.

Nils Reimers and Iryna Gurevych. Sentence-bert: Sentence embeddings using siamese bert-networks. In *Proceedings of the 2019 Conference on Empirical Methods in Natural Language Processing and the 9th International Joint Conference on Natural Language Processing (EMNLP-IJCNLP)*, pp. 3982–3992, 2019.

Nils Reimers, Philip Beyer, and Iryna Gurevych. Task-oriented intrinsic evaluation of semantic textual similarity. In *Proceedings of COLING 2016, the 26th International Conference on Computational Linguistics: Technical Papers*, pp. 87–96, 2016.

Olga Russakovsky, Jia Deng, Hao Su, Jonathan Krause, Sanjeev Satheesh, Sean Ma, Zhiheng Huang, Andrej Karpathy, Aditya Khosla, Michael Bernstein, et al. Imagenet large scale visual recognition challenge. *International journal of computer vision*, 115(3):211–252, 2015.

Richard Socher, Alex Perelygin, Jean Wu, Jason Chuang, Christopher D Manning, Andrew Y Ng, and Christopher Potts. Recursive deep models for semantic compositionality over a sentiment treebank. In *Proceedings of the 2013 conference on empirical methods in natural language processing*, pp. 1631–1642, 2013.

Jianlin Su, Jiarun Cao, Weijie Liu, and Yangyiwen Ou. Whitening sentence representations for better semantics and faster retrieval. *arXiv preprint arXiv:2103.15316*, 2021.

Joseph John Thomson. Xxiv. on the structure of the atom: an investigation of the stability and periods of oscillation of a number of corpuscles arranged at equal intervals around the circumference of a circle; with application of the results to the theory of atomic structure. *The London, Edinburgh, and Dublin Philosophical Magazine and Journal of Science*, 7(39):237–265, 1904.

Ellen M Voorhees and Dawn M Tice. Building a question answering test collection. In *Proceedings of the 23rd annual international ACM SIGIR conference on Research and development in information retrieval*, pp. 200–207, 2000.

Tongzhou Wang and Phillip Isola. Understanding contrastive representation learning through alignment and uniformity on the hypersphere. In *International Conference on Machine Learning*, pp. 9929–9939. PMLR, 2020.

Kilian Q Weinberger and Lawrence K Saul. Distance metric learning for large margin nearest neighbor classification. *Journal of Machine Learning Research*, 10:207–244, 2009.

Janyce Wiebe, Theresa Wilson, and Claire Cardie. Annotating expressions of opinions and emotions in language. *Language resources and evaluation*, 39(2):165–210, 2005.

Xing Wu, Chaochen Gao, Liangjun Zang, Jizhong Han, Zhongyuan Wang, and Songlin Hu. Esimcse: Enhanced sample building method for contrastive learning of unsupervised sentence embedding. *arXiv preprint arXiv:2109.04380*, 2021.

Zhirong Wu, Yuanjun Xiong, Stella X Yu, and Dahua Lin. Unsupervised feature learning via non-parametric instance discrimination. In *Proceedings of the IEEE conference on computer vision and pattern recognition*, pp. 3733–3742, 2018.

Yuanmeng Yan, Rumei Li, Sirui Wang, Fuzheng Zhang, Wei Wu, and Weiran Xu. Consert: A contrastive framework for self-supervised sentence representation transfer. In *Proceedings of the 59th Annual Meeting of the Association for Computational Linguistics and the 11th International Joint Conference on Natural Language Processing (Volume 1: Long Papers)*, pp. 5065–5075, 2021.

Chun-Hsiao Yeh, Cheng-Yao Hong, Yen-Chi Hsu, Tyng-Luh Liu, Yubei Chen, and Yann LeCun. Decoupled contrastive learning. *arXiv preprint arXiv:2110.06848*, 2021.

Hongyi Zhang, Moustapha Cisse, Yann N Dauphin, and David Lopez-Paz. mixup: Beyond empirical risk minimization. In *International Conference on Learning Representations*, 2018.

Miaoran Zhang, Marius Mosbach, David Adelani, Michael Hedderich, and Dietrich Klakow. MCSE: Multimodal contrastive learning of sentence embeddings. In *Proceedings of the 2022 Conference of the North American Chapter of the Association for Computational Linguistics: Human Language Technologies*, pp. 5959–5969, Seattle, United States, July 2022a. Association for Computational Linguistics. doi: 10.18653/v1/2022.naacl-main.436. URL `https://aclanthology.org/2022.naacl-main.436`.

Yanzhao Zhang, Richong Zhang, Samuel Mensah, Xudong Liu, and Yongyi Mao. Unsupervised sentence representation via contrastive learning with mixing negatives. In *Proceedings of the AAAI Conference on Artificial Intelligence*, volume 36, pp. 8220–8230, 2022b.

Yuhao Zhang, Hongji Zhu, Yongliang Wang, Nan Xu, Xiaobo Li, and Binqiang Zhao. A contrastive framework for learning sentence representations from pairwise and triple-wise perspective in angular space. In *Proceedings of the 60th Annual Meeting of the Association for Computational Linguistics (Volume 1: Long Papers)*, pp. 4892–4903, 2022c.

Kun Zhou, Beichen Zhang, Wayne Xin Zhao, and Ji-Rong Wen. Debiased contrastive learning of unsupervised sentence representations. In *Proceedings of the 60th Annual Meeting of the Association for Computational Linguistics (Volume 1: Long Papers)*, pp. 6120–6130, 2022.

A Experiment Details

A.1 Experiment Setup

Following recent works in SRL Gao et al. (2021); Yan et al. (2021); Zhang et al. (2022b), we use the SentEval toolkit Conneau & Kiela (2018) to evaluate the quality of sentence representations.

For intrinsic evaluation, i.e., correlation to human judgments, we use seven Semantic Textual Similarity (STS) datasets (STS12-16 Agirre et al. (2012; 2013; 2014; 2015; 2016), STS-B Cer et al. (2017) and SICK-R Marelli et al. (2014) in SentEval. For extrinsic evaluation, i.e., transfer ability to downstream tasks, we also select seven downstream task datasets (MR Pang & Lee (2005), CR Hu & Liu (2004), SUBJ Pang & Lee (2004), MPQA Wiebe et al. (2005), SST-2 Socher et al. (2013), TREC Voorhees & Tice (2000) and MRPC Dolan & Brockett (2005)) to verify the migration ability of the sentence representations. We followed the default configuration recommended by SentEval for training and evaluation.

A.2 TRAINING DETAILS

We validate the effectiveness of all loss functions based on the SimCSE Gao et al. (2021) as it is effective but simple enough, so the performance is not easily influenced by other factors.

Following Gao et al. (2021), we observe the following points during training: (1) No data in any STS training set is used for training; (2) 1,000,000 sentences sampled from the English Wikipedia[3] are used for training instead; (3) Spearman correlation on STS-B development set is recorded each 125 steps; (4) The checkpoints corresponding to the highest Spearman correlation will be saved for evaluation; (5) The training period is one epoch for all pretrained models.

We implement the codes using Python3.7 and Pytorch1.12.0 and experiment with the single 32G NVIDIA V100 GPU.

Method	Parameter	$\text{BERT}_{\text{base}}$	$\text{BERT}_{\text{large}}$	$\text{RoBERTa}_{\text{base}}$	$\text{RoBERTa}_{\text{large}}$
$\mathcal{L}_{cl}$	τ	0.05	0.05	0.05	0.05
	learning rate	1e-5	1e-5	1e-5	1e-5
	batch size	64	64	128	128
$\mathcal{L}_{\text{a\&u}}$	α	2	2	2	2
	t	6	6	6	6
	λ	0.1	0.1	0.2	0.4
	learning rate	1e-5	1e-5	1e-5	1e-5
	batch size	64	64	64	64
$\mathcal{L}_{\text{dcl}}$	τ	0.03	0.01	0.02	0.02
	learning rate	1e-5	5e-5	1e-5	1e-5
	batch size	64	64	64	64
$\mathcal{L}_{\text{dcl+}}$	τ	0.17	0.18	0.15	0.17
	learning rate	3e-5	5e-5	1e-5	1e-5
	batch size	64	64	64	64
$\mathcal{L}_{\text{mpt}}$	m	0.23	0.24	0.29	0.31
	learning rate	1e-5	1e-5	7e-6	7e-6
	batch size	64	64	64	64
$\mathcal{L}_{\text{met}}$	m	0.45	0.50	0.43	0.45
	learning rate	1e-5	1e-5	7e-6	7e-6
	batch size	128	128	128	128
$\mathcal{L}_{\text{mat}}$	m	0.15π	0.17π	0.14π	0.13π
	learning rate	1e-5	3e-5	7e-6	7e-6
	batch size	128	128	128	128

Table 2: The parameters corresponding to the best results of the STS tasks, which are also corresponding to the reported results and the plotted figures in this paper.

A.3 PARAMETER SETTING

For all loss functions, we perform a grid search on learning rate ={7e-6, 1e-5, 3e-5, 5e-5} and batch size ={64, 128, 256, 512}. For other hyperparameters in every optimization objectives, we first narrow the interval via an extensive search, then the grid search is conducted in the following ranges:

- $\mathcal{L}_{\text{cl}}$ and $\mathcal{L}_{\text{dcl}}$
  - $\tau = \{0.03, 0.05, 0.07\}$
- $\mathcal{L}_{\text{a\&u}}$
  - $\lambda = \{0.1, 0.3, 0.5, 0.7, 0.9\}$

[3]https://huggingface.co/datasets/princeton-nlp/datasets-for-simcse/resolve/main/wiki1m_for_simcse.txt

  - $\alpha = \{1.0, 2.0, 3.0\}$
  - $t \in [2, 10]$, step size is 1
- $\mathcal{L}_{\text{dcl+}}$
  - $\tau \in [0.10, 0.20]$, step size is 0.01
- $\mathcal{L}_{\text{mpt}}$
  - $m \in [0.20, 0.35]$, step size is 0.01
- $\mathcal{L}_{\text{met}}$
  - $m \in [0.40, 0.50]$, step size is 0.01
- $\mathcal{L}_{\text{mat}}$
  - $m \in \{0.10\pi, 0.20\pi]$, step size is 0.01π

The optimal parameters are shown in Table 2, which are adopted to report all results and plot to all the images in this paper.

A.4 Evaluation Protocol

We report the performance of the sentence representation on the STS task using the Spearman's rank correlation, which has been widely used in recent work. Compared with the Pearson correlation, Spearman's rank correlation focuses on relative Ranking instead of absolute scores, which is more in line with practical retrieval applications of text similarity matching Reimers et al. (2016).

B The Analysis on Uniformity Part

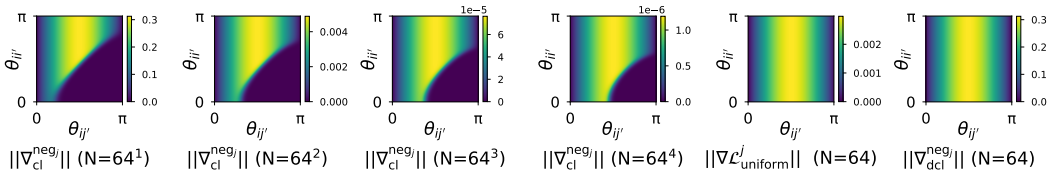

(a) Comparison between contrastive loss and its decoupled forms in the *uniformity* part of the gradient norm.

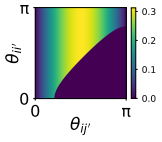

(b) The *uniformity* part of the gradient norm for $\mathcal{L}_{\text{dcl+}}$.

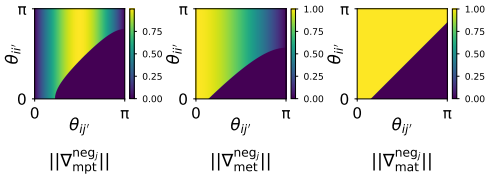

(c) Comparsion among three loss functions like Tripet Loss in the *uniformity* part of the gradient norm. The horizontal axis represents the minimum angle between the anchor and the negative samples.

Figure 4: Gradient norms of all the loss functions studied in the main text with respect to the *uniformity* part. All plotted images ignore $1/\|h_i\|$ and reflect only the gradient contribution of a single negative sample to the anchor.

Similar to the main text, we study the *uniformity* part of the gradient norm of all the loss functions mentioned in the main text, and their formulas are shown below:

$$\left\|\nabla^{\text{neg}_{\text{j}}}_{\text{cl}}\right\| = \frac{1}{\tau} \frac{\exp\left(\cos\theta_{ij'}/\tau\right)\sin\theta_{ij'}}{\exp\left(\cos\theta_{ii'}/\tau\right) + \sum_{j,j\neq i}^{N}\exp\left(\cos\theta_{ij'}/\tau\right)} \frac{1}{\|h_i\|} \tag{16}$$

$$\left\|\nabla\mathcal{L}^{j}_{\text{uniform}}\right\| = \frac{2t\exp\left(2t\cos(\theta_{ij'})\right)\sin\theta_{ij'}}{\sum_{i}^{N}\sum_{j,j\neq i}^{N}\exp\left(2t\cos(\theta_{ij'})\right)} \frac{1}{\|h_i\|} \tag{17}$$

$$\left\|\nabla_{\mathrm{dcl}}^{\mathrm{neg}_j}\right\| = \frac{1}{\tau}\frac{\exp\left(\cos\theta_{ij'}/\tau\right)\sin\theta_{ij'}}{\sum_{j,j\neq i}^{N}\exp\left(\cos\theta_{ij'}/\tau\right)}\frac{1}{\|h_i\|} \tag{18}$$

$$\left\|\nabla_{\mathrm{dcl+}}^{\mathrm{pos}}\right\| = \begin{cases} \frac{1}{\tau}\frac{\exp\left(\cos\theta_{ij'}/\tau\right)\sin\theta_{ij'}}{\sum_{j,j\neq i}^{N}\exp\left(\cos\theta_{ij'}/\tau\right)}\frac{1}{\|h_i\|}, & \hat{h}_i^T\hat{h}_i'/\tau - \log\sum_{j,j\neq i}^{N}\exp\left(\hat{h}_i^T\hat{h}_j'\right)/\tau < 0 \\ 0, & \hat{h}_i^T\hat{h}_i'/\tau - \log\sum_{j,j\neq i}^{N}\exp\left(\hat{h}_i^T\hat{h}_j'\right)/\tau \geq 0 \end{cases} \tag{19}$$

$$\left\|\nabla_{\mathrm{mpt}}^{\mathrm{pos}}\right\| = \begin{cases} \frac{\sin\left(\theta_{ij'}\right)}{\|h_i\|}, & \hat{h}_i^T\hat{h}_i' + \max_{j,j\neq i}\hat{h}_i^T\hat{h}_j < m \\ 0, & \hat{h}_i^T\hat{h}_i' + \max_{j,j\neq i}\hat{h}_i^T\hat{h}_j \geq m \end{cases} \tag{20}$$

$$\|\nabla_{\mathrm{met}}^{\mathrm{pos}}\| = \begin{cases} \frac{\cos\left(\theta_{ij'}/2\right)}{\|h_i\|}, & \|\hat{h}_i - \hat{h}_i'\|_2 - \min_{j,j\neq i}\|\hat{h}_i - \hat{h}_j'\|_2 < m \\ 0, & \|\hat{h}_i - \hat{h}_i'\|_2 - \min_{j,j\neq i}\|\hat{h}_i - \hat{h}_j'\|_2 \geq m \end{cases} \tag{21}$$

$$\|\nabla_{\mathrm{mat}}^{\mathrm{pos}}\| = \begin{cases} \frac{1}{\|h_i\|}, & \theta_{ii'} - \min_{j,j\neq i}\theta_{ij'} < m \\ 0, & \theta_{ii'} - \min_{j,j\neq i}\theta_{ij'} \geq m \end{cases} \tag{22}$$

The derivation of all the above equations can be found in Appendix C, and their trends with $\theta_{ii'}$-$\theta_{ij'}$ are plotted in Figure 4. The findings of the *uniformity* part is highly similar to those of the *alignment* part:

- $\|\nabla_{\mathrm{cl}}^{\mathrm{neg_j}}\|$ approaches $\|\nabla\mathcal{L}_{\mathrm{uniform}}^{j}\|$ and $\|\nabla_{\mathrm{dcl}}^{\mathrm{neg}_j}\|$ as the number of negative samples increases.
- When the number of negative samples is small, "gradient dissipation" exists for $\|\nabla_{\mathrm{cl}}^{\mathrm{neg_j}}\|$, while $\|\nabla\mathcal{L}_{\mathrm{uniform}}^{j}\|$ and $\|\nabla_{\mathrm{dcl}}^{\mathrm{neg}_j}\|$ do not exist.
- $\|\nabla_{\mathrm{dcl+}}^{\mathrm{neg}_j}\|$ exists the similar "gradient dissipation" property of $\|\nabla_{\mathrm{cl}}^{\mathrm{neg_j}}\|$.
- $\|\nabla_{\mathrm{mpt}}^{\mathrm{pos}}\|$, $\|\nabla_{\mathrm{met}}^{\mathrm{pos}}\|$ and $\|\nabla_{\mathrm{mat}}^{\mathrm{pos}}\|$ also exist the propety of "gradient dissipation", but differs from $\|\nabla_{\mathrm{cl}}^{\mathrm{neg_j}}\|$ in the trend of the gradient norms.

C Formula Derivation

C.1 The derivation of Equation 6

$$\begin{aligned}
\frac{\partial\mathcal{L}_{\mathrm{cl}}}{\partial h_i} &= -\frac{1}{\tau}\left(\hat{h}_i' + \frac{\exp\left(\hat{h}_i^T\hat{h}_i'/\tau\right)\hat{h}_i' + \sum_{j,j\neq i}^{N}\exp\left(\hat{h}_i^T\hat{h}_j'/\tau\right)\hat{h}_j'}{\exp\left(\hat{h}_i^T\hat{h}_i'/\tau\right) + \sum_{j,j\neq i}^{N}\exp\left(\hat{h}_i^T\hat{h}_j'/\tau\right)}\right)\frac{\partial\hat{h}_i}{\partial h_i} \\
&= -\frac{1}{\tau}\frac{\sum_{j,j\neq i}^{N}\exp\left(\hat{h}_i^T\hat{h}_j'/\tau\right)\left(\hat{h}_i' - \hat{h}_j'\right)}{\exp\left(\hat{h}_i^T\hat{h}_i'/\tau\right) + \sum_{j,j\neq i}^{N}\exp\left(\hat{h}_i^T\hat{h}_j'/\tau\right)}\frac{I - M_{h_i}}{\|h_i\|} \\
&= -\frac{1}{\tau}\sum_{j,j\neq i}^{N}\frac{\exp\left(\hat{h}_i^T\hat{h}_j'/\tau\right)\left(\hat{h}_i' - \hat{h}_i - \left(\hat{h}_j' - \hat{h}_i\right)\right)}{\exp\left(\hat{h}_i^T\hat{h}_i'/\tau\right) + \sum_{j,j\neq i}^{N}\exp\left(\hat{h}_i^T\hat{h}_j'/\tau\right)}\frac{I - M_{h_i}}{\|h_i\|} \\
&= \underbrace{-\frac{1}{\tau}\frac{\sum_{j,j\neq i}^{N}\exp\left(\hat{h}_i^T\hat{h}_j'/\tau\right)\left(\hat{h}_i' - \hat{h}_i\right)}{\exp\left(\hat{h}_i^T\hat{h}_i'/\tau\right) + \sum_{j,j\neq i}^{N}\exp\left(\hat{h}_i^T\hat{h}_j'/\tau\right)}\frac{I - M_{h_i}}{\|h_i\|}}_{\nabla_{\mathrm{cl}}^{\mathrm{pos}}} \\
&\quad + \underbrace{\frac{1}{\tau}\frac{\sum_{j,j\neq i}^{N}\exp\left(\hat{h}_i^T\hat{h}_j'/\tau\right)\left(\hat{h}_j' - \hat{h}_i\right)}{\exp\left(\hat{h}_i^T\hat{h}_i'/\tau\right) + \sum_{j,j\neq i}^{N}\exp\left(\hat{h}_i^T\hat{h}_j'/\tau\right)}\frac{I - M_{h_i}}{\|h_i\|}}_{\sum_{j,j\neq i}^{N}\nabla_{\mathrm{cl}}^{\mathrm{neg}_j}}
\end{aligned} \tag{23}$$

C.2 THE DERIVATION OF EQUATION 7 AND EQUATION 16

$$
\begin{aligned}
\|\nabla_{\mathrm{cl}}^{\mathrm{pos}}\| &= \left\| -\frac{1}{\tau} \frac{\sum_{j,j\neq i}^{N} \exp\left(\hat{h}_i^T \hat{h}_j'/\tau\right)\left(\hat{h}_i' - \hat{h}_i\right)}{\exp\left(\hat{h}_i^T \hat{h}_i'/\tau\right) + \sum_{j,j\neq i}^{N} \exp\left(\hat{h}_i^T \hat{h}_j'/\tau\right)} \frac{I - M_{h_i}}{\|h_i\|} \right\| \\
&= \frac{1}{\tau} \frac{\sum_{j,j\neq i}^{N} \exp\left(\hat{h}_i^T \hat{h}_j'/\tau\right)}{\exp\left(\hat{h}_i^T \hat{h}_i'/\tau\right) + \sum_{j,j\neq i}^{N} \exp\left(\hat{h}_i^T \hat{h}_j'/\tau\right)} \frac{\left\|\left(\hat{h}_i' - \hat{h}_i\right)(I - M_{h_i})\right\|}{\|h_i\|} \\
&= \frac{1}{\tau} \frac{\sum_{j,j\neq i}^{N} \exp\left(\cos\theta_{ij'}/\tau\right)}{\exp\left(\cos\theta_{ii'}/\tau\right) + \sum_{j,j\neq i}^{N} \exp\left(\cos\theta_{ij'}/\tau\right)} \frac{\left\|\hat{h}_i' - \hat{h}_i \cos\theta_{ij'}\right\|}{\|h_i\|} \\
&= \frac{1}{\tau} \frac{\sum_{j,j\neq i}^{N} \exp\left(\cos\theta_{ij'}/\tau\right)\sin\theta_{ii'}}{\exp\left(\cos\theta_{ii'}/\tau\right) + \sum_{j,j\neq i}^{N} \exp\left(\cos\theta_{ij'}/\tau\right)} \frac{1}{\|h_i\|}
\end{aligned}
\tag{24}
$$

$$
\begin{aligned}
\left\|\nabla_{\mathrm{cl}}^{\mathrm{neg}_j}\right\| &= \left\| \frac{1}{\tau} \frac{\exp\left(\hat{h}_i^T \hat{h}_j'/\tau\right)\left(\hat{h}_j' - \hat{h}_i\right)}{\exp\left(\hat{h}_i^T \hat{h}_i'/\tau\right) + \sum_{j,j\neq i}^{N} \exp\left(\hat{h}_i^T \hat{h}_j'/\tau\right)} \frac{I - M_{h_i}}{\|h_i\|} \right\| \\
&= \frac{1}{\tau} \frac{\exp\left(\hat{h}_i^T \hat{h}_j'/\tau\right)}{\exp\left(\hat{h}_i^T \hat{h}_i'/\tau\right) + \sum_{j,j\neq i}^{N} \exp\left(\hat{h}_i^T \hat{h}_j'/\tau\right)} \frac{\left\|\left(\hat{h}_j' - \hat{h}_i\right)(I - M_{h_i})\right\|}{\|h_i\|} \\
&= \frac{1}{\tau} \frac{\exp\left(\cos\theta_{ij'}/\tau\right)}{\exp\left(\cos\theta_{ii'}/\tau\right) + \sum_{j,j\neq i}^{N} \exp\left(\cos\theta_{ij'}/\tau\right)} \frac{\left\|\hat{h}_j' - \hat{h}_i \cos\theta_{ij'}\right\|}{\|h_i\|} \\
&= \frac{1}{\tau} \frac{\exp\left(\cos\theta_{ij'}/\tau\right)\sin\theta_{ij'}}{\exp\left(\cos\theta_{ii'}/\tau\right) + \sum_{j,j\neq i}^{N} \exp\left(\cos\theta_{ij'}/\tau\right)} \frac{1}{\|h_i\|}
\end{aligned}
\tag{25}
$$

C.3 THE DERIVATION OF EQUATION 8 AND 17

$$
\mathcal{L}_{\mathrm{align}} = \left(\left\|\hat{h}_i - \hat{h}_i'\right\|_2^2\right)^{\frac{\alpha}{2}} = \left(2 - 2\hat{h}_i^T \hat{h}_i'\right)^{\frac{\alpha}{2}}
\tag{26}
$$

$$
\begin{aligned}
\frac{\partial \mathcal{L}_{\mathrm{align}}}{\partial h_i} &= \frac{\alpha}{2}\left(2 - 2\hat{h}_i^T \hat{h}_i'\right)^{\frac{\alpha-2}{2}} (-2\hat{h}_i') \frac{I - M_{h_i}}{\|h_i\|} \\
&= -\alpha\left(2 - 2\hat{h}_i^T \hat{h}_i'\right)^{\frac{\alpha-2}{2}} \hat{h}_i' \frac{I - M_{h_i}}{\|h_i\|}
\end{aligned}
\tag{27}
$$

$$
\begin{aligned}
\left\|\frac{\partial \mathcal{L}_{\mathrm{align}}}{\partial h_i}\right\| &= \alpha(2 - 2\cos\theta_{ii'})^{\frac{\alpha-2}{2}} \frac{\left\|\hat{h}_i' - \hat{h}_i \cos\theta_{ii'}\right\|}{\|h_i\|} \\
&= \alpha(4\sin^2(\theta_{ii'}/2))^{\frac{\alpha-2}{2}} \sin\theta_{ii'} \frac{1}{\|h_i\|} \\
&= \alpha(2\sin(\theta_{ii'}/2))^{\alpha-2} \sin\theta_{ii'} \frac{1}{\|h_i\|} \\
&= \|\nabla \mathcal{L}_{\mathrm{align}}\|
\end{aligned}
\tag{28}
$$

$$
\mathcal{L}_{\mathrm{uniform}} = \log \frac{1}{N(N-1)} \sum_{i}^{N} \sum_{j,j\neq i}^{N} \exp\left(-t\left\|\hat{h}_i - \hat{h}_j'\right\|_2^2\right)
\tag{29}
$$

$$
\begin{aligned}
\frac{\partial \mathcal{L}_{\text{uniform}}}{\partial h_i} &= \frac{2t \sum_i^N \sum_{j,j\neq i}^N \exp\left(-t \left\|\hat{h}_i - \hat{h}'_j\right\|_2^2\right) \hat{h}'_j}{\sum_i^N \sum_{j,j\neq i}^N \exp\left(-t \left\|\hat{h}_i - \hat{h}'_j\right\|_2^2\right)} \frac{I - M_{h_i}}{\|h_i\|} \\
&= \frac{2t \sum_i^N \sum_{j,j\neq i}^N \exp\left(-t \left\|\hat{h}_i - \hat{h}'_j\right\|_2^2\right) \left(\hat{h}'_j - \hat{h}_i\right)}{\sum_i^N \sum_{j,j\neq i}^N \exp\left(-t \left\|\hat{h}_i - \hat{h}'_j\right\|_2^2\right)} \frac{I - M_{h_i}}{\|h_i\|} \\
&= \sum_i^N \sum_{j,j\neq i}^N \nabla \mathcal{L}_{\text{uniform}}^j
\end{aligned} \tag{30}
$$

$$
\begin{aligned}
\left\|\nabla \mathcal{L}_{\text{uniform}}^j\right\| &= \left\| \frac{2t \exp\left(-t \left\|\hat{h}_i - \hat{h}'_j\right\|_2^2\right) \left(\hat{h}'_j - \hat{h}_i\right)}{\sum_i^N \sum_{j,j\neq i}^N \exp\left(-t \left\|\hat{h}_i - \hat{h}'_j\right\|_2^2\right)} \frac{I - M_{h_i}}{\|h_i\|} \right\| \\
&= \frac{2t \exp\left(-4t \sin^2(\theta_{ij'}/2)\right)}{\sum_i^N \sum_{j,j\neq i}^N \exp\left(-4t \sin^2(\theta_{ij'}/2)\right)} \frac{\left\|\left(\hat{h}'_j - \hat{h}_i\right)(I - M_{h_i})\right\|}{\|h_i\|} \\
&= \frac{2t \exp\left(-4t \sin^2(\theta_{ij'}/2)\right)}{\sum_i^N \sum_{j,j\neq i}^N \exp\left(-4t \sin^2(\theta_{ij'}/2)\right)} \frac{\left\|\hat{h}'_j - \hat{h}_i \cos\theta_{ij'}\right\|}{\|h_i\|} \\
&= \frac{2t \exp\left(-4t \sin^2(\theta_{ij'}/2)\right) \sin\theta_{ij'}}{\sum_i^N \sum_{j,j\neq i}^N \exp\left(-4t \sin^2(\theta_{ij'}/2)\right)} \frac{1}{\|h_i\|}
\end{aligned} \tag{31}
$$

C.4 The derivation of Equation 9, 11, 18 and 19

$$
\frac{\partial \mathcal{L}_{\text{dcl}}}{\partial h_i} = \underbrace{-\frac{\hat{h}'_i - \hat{h}_i}{\tau} \frac{I - M_{h_i}}{\|h_i\|}}_{\nabla_{\text{dcl}}^{\text{pos}}} + \underbrace{\frac{1}{\tau} \frac{\sum_{j,j\neq i}^N \exp\left(\hat{h}_i^T \hat{h}'_j/\tau\right) \left(\hat{h}'_j - \hat{h}_i\right)}{\sum_{j,j\neq i}^N \exp\left(\hat{h}_i^T \hat{h}'_j/\tau\right)} \frac{I - M_{h_i}}{\|h_i\|}}_{\sum_{j,j\neq i}^N \nabla_{dcl}^{neg_j}} \tag{32}
$$

$$
\|\nabla_{\text{dcl}}^{\text{pos}}\| = \left\| \frac{1}{\tau} \frac{\left(\hat{h}'_j - \hat{h}_i\right)(I - M_{h_i})}{\|h_i\|} \right\| = \frac{1}{\tau} \frac{\left\|\left(\hat{h}'_j - \hat{h}_i\right)(I - M_{h_i})\right\|}{\|h_i\|} = \frac{1}{\tau} \frac{\sin\theta_{ij'}}{\|h_i\|} \tag{33}
$$

$$
\begin{aligned}
\left\|\nabla_{\text{dcl}}^{\text{neg}_j}\right\| &= \left\| \frac{1}{\tau} \frac{\exp\left(\hat{h}_i^T \hat{h}'_j/\tau\right) \left(\hat{h}'_j - \hat{h}_i\right)}{\sum_{j,j\neq i}^N \exp\left(\hat{h}_i^T \hat{h}'_j/\tau\right)} \frac{I - M_{h_i}}{\|h_i\|} \right\| \\
&= \frac{1}{\tau} \frac{\exp\left(\hat{h}_i^T \hat{h}'_j/\tau\right)}{\sum_{j,j\neq i}^N \exp\left(\hat{h}_i^T \hat{h}'_j/\tau\right)} \frac{\left\|\left(\hat{h}'_j - \hat{h}_i\right)(I - M_{h_i})\right\|}{\|h_i\|} \\
&= \frac{1}{\tau} \frac{\exp\left(\cos\theta_{ij'}/\tau\right)}{\sum_{j,j\neq i}^N \exp\left(\cos\theta_{ij'}/\tau\right)} \frac{\left\|\hat{h}'_j - \hat{h}_i \cos\theta_{ij'}\right\|}{\|h_i\|} \\
&= \frac{1}{\tau} \frac{\exp\left(\cos\theta_{ij'}/\tau\right) \sin\theta_{ij'}}{\sum_{j,j\neq i}^N \exp\left(\cos\theta_{ij'}/\tau\right)} \frac{1}{\|h_i\|}
\end{aligned} \tag{34}
$$

C.5 THE DERIVATION OF EQUATION 12

$$
\begin{aligned}
\mathcal{L}_{\mathrm{cl}} &= -\log \frac{\exp\left(\hat{h}_i^T \hat{h}_i'/\tau\right)}{\exp\left(\hat{h}_i^T \hat{h}_i'/\tau\right) + \sum_j^N \exp\left(\hat{h}_i^T \hat{h}_j'/\tau\right)\Big)} \\
&= \log\left(1 + \frac{\sum_j^N \exp\left(\hat{h}_i^T \hat{h}_j'/\tau\right)}{\exp\left(\hat{h}_i^T \hat{h}_i'/\tau\right)}\right) \\
&= \log\left(1 + \exp\left(-\hat{h}_i^T \hat{h}_i'/\tau\right) \sum_{\mathrm{j}, j\neq i}^{N} \exp\left(\hat{h}_i^T \hat{h}_j'/\tau\right)\right) \\
&= \log\left(1 + \exp\left(-\hat{h}_i^T \hat{h}_i'/\tau + \log \sum_{j, j\neq i}^{N} \exp\left(\hat{h}_i^T \hat{h}_j'/\tau\right)\right)\right) \\
&\leq \log 2 + \max\left(-\hat{h}_i^T \hat{h}_i'/\tau + \log \sum_{j, j\neq i}^{N} \exp\left(\hat{h}_i^T \hat{h}_j'/\tau\right), 0\right) \\
&\leq \log 2 + \max\left(-\hat{h}_i^T \hat{h}_i'/\tau + \log\left[(N-1) \max_{j, j\neq i} \exp\left(\hat{h}_i^T \hat{h}_j'/\tau\right)\right], 0\right) \\
&= \log 2 + \max\left(-\hat{h}_i^T \hat{h}_i'/\tau + \max_{j, j\neq i}\left(\hat{h}_i^T \hat{h}_j\right)/\tau + \log(N-1), 0\right) \\
&= \log 2 + \frac{1}{\tau} \max\left(-\hat{h}_i^T \hat{h}_i' + \max_{j, j\neq i}\left(\hat{h}_i^T \hat{h}_j\right) + \tau \log(N-1), 0\right)
\end{aligned}
\tag{35}
$$

where the basis for the first inequality sign is

$$
\begin{aligned}
f(x) &= \log(1 + \exp(\mathrm{x})) \\
&= \log\left(\sum_{\mathrm{t}\in\{0,\mathrm{x}\}} \exp(\mathrm{t})\right) \\
&\leq \log(2\exp(\max(\mathrm{t}))) \\
&= \log 2 + \max(x, 0)
\end{aligned}
\tag{36}
$$

C.6 THE DERIVATION OF $\left\|\nabla_{mpt}^{pos}\right\|$, $\|\nabla_{met}^{pos}\|$, $\|\nabla_{mat}^{pos}\|$, $\left\|\nabla_{mpt}^{neg^j}\right\|$, $\left\|\nabla_{met}^{neg^j}\right\|$ AND $\left\|\nabla_{mat}^{neg^j}\right\|$

Consider a generic form of the optimization objective first:

$$
\mathcal{L}_{\mathrm{mdt}} = \max\left(0, \rho\left(\hat{h}_i, \hat{h}_i'\right) - \min_{j, j\neq i} \rho\left(\hat{h}_i, \hat{h}_j'\right) + m\right) \tag{37}
$$

where $\rho(.,.)$ represents a function used to calculate the similarity. Then the gradient of $\mathcal{L}_{\mathrm{mdt}}$ with respect to h_i is calculated and decomposed:

$$
\frac{\partial \mathcal{L}_{\mathrm{mdt}}}{\partial h_i} = \begin{cases} \underbrace{\frac{\partial \rho\left(\hat{h}_i, \hat{h}_i'\right)}{\partial h_i} \frac{I - M_{h_i}}{\|h_i\|}}_{\nabla_{\mathrm{mdt}}^{\mathrm{pos}}} - \underbrace{\frac{\partial \min_{j, j\neq i} \rho\left(\hat{h}_i, \hat{h}_j'\right)}{\partial h_i} \frac{I - M_{h_i}}{\|h_i\|}}_{\nabla_{\mathrm{mdt}}^{\mathrm{neg}}}, & \rho\left(\hat{h}_i, \hat{h}_i'\right) - \min_{j, j\neq i} \rho\left(\hat{h}_i, \hat{h}_j'\right) < m \\ 0, & \rho\left(\hat{h}_i, \hat{h}_i'\right) - \min_{j, j\neq i} \rho\left(\hat{h}_i, \hat{h}_j'\right) \geq m \end{cases} \tag{38}
$$

where $\nabla_{\mathrm{mdt}}^{\mathrm{neg}}$ is only contributed by the negative sample with the closest distance to the anchor point. By specifying $\rho(.,.)$ as dot product, l_2-norm and angle, we can get the gradient norm of $\mathcal{L}_{\mathrm{mpt}}$, $\mathcal{L}_{\mathrm{met}}$ and $\mathcal{L}_{\mathrm{mat}}$ with respect to the part of *alignment* respectively:

$$\|\nabla_{\text{mdt}}^{\text{pos}}\| = \begin{cases} \dfrac{\sin(\theta_{ii'})}{\|h_i\|}, & \rho(\hat{h}_i, \hat{h}_i') = \hat{h}_i^T \hat{h}_i' \quad and \quad \rho\left(\hat{h}_i, \hat{h}_i'\right) - \min\limits_{j,j\neq i} \rho\left(\hat{h}_i, \hat{h}_j'\right) < m \\ \dfrac{\cos(\theta_{ii'}/2)}{\|h_i\|}, & \rho(\hat{h}_i, \hat{h}_i') = -\left\|\hat{h}_i - \hat{h}_i'\right\|_2 \quad and \quad \rho\left(\hat{h}_i, \hat{h}_i'\right) - \min\limits_{j,j\neq i} \rho\left(\hat{h}_i, \hat{h}_j'\right) < m \\ \dfrac{1}{\|h_i\|}, & \rho(\hat{h}_i, \hat{h}_i') = -\theta_{ij'} \quad and \quad \rho\left(\hat{h}_i, \hat{h}_i'\right) - \min\limits_{j,j\neq i} \rho\left(\hat{h}_i, \hat{h}_j'\right) < m \\ 0, & \rho\left(\hat{h}_i, \hat{h}_i'\right) - \min\limits_{j,j\neq i} \rho\left(\hat{h}_i, \hat{h}_j'\right) \geq m \end{cases} \tag{39}$$

Similarly, we can derive the gradient norm of each loss function corresponding to the part of *uniformity* respectively:

$$\|\nabla_{\text{mdt}}^{\text{neg}}\| = \begin{cases} \dfrac{\sin(\min\limits_{j,j\neq i} \theta_{ij'})}{\|h_i\|}, & \rho(\hat{h}_i, \hat{h}_j') = \hat{h}_i^T \hat{h}_j' \quad and \quad \rho\left(\hat{h}_i, \hat{h}_i'\right) - \min\limits_{j,j\neq i} \rho\left(\hat{h}_i, \hat{h}_j'\right) < m \\ \dfrac{\cos(\min\limits_{j,j\neq i} \theta_{ij'}/2)}{\|h_i\|}, & \rho(\hat{h}_i, \hat{h}_j') = -\left\|\hat{h}_i - \hat{h}_j'\right\|_2 \quad and \quad \rho\left(\hat{h}_i, \hat{h}_i'\right) - \min\limits_{j,j\neq i} \rho\left(\hat{h}_i, \hat{h}_j'\right) \geq m \\ \dfrac{1}{\|h_i\|}, & \rho(\hat{h}_i, \hat{h}_j') = -\theta_{ij'} \quad and \quad \rho\left(\hat{h}_i, \hat{h}_i'\right) - \min\limits_{j,j\neq i} \rho\left(\hat{h}_i, \hat{h}_j'\right) < m \\ 0, & \rho\left(\hat{h}_i, \hat{h}_i'\right) - \min\limits_{j,j\neq i} \rho\left(\hat{h}_i, \hat{h}_j'\right) \geq m \end{cases} \tag{40}$$

D THE CONNECTION BETWEEN THE TWO DECOUPLE FORMS

In this paper, two important research objectives are two decoupled forms of contrastive loss. The first one is the alignment and uniformity proposed by Wang & Isola (2020):

$$\mathcal{L}_{\text{align}}(f;\alpha) \triangleq \mathop{\mathbb{E}}_{(\hat{h}_i, \hat{h}_i') \sim p_{\text{pos}}} \left[\|\hat{h}_i - \hat{h}_i'\|_2^{\alpha}\right], \quad \alpha > 0 \tag{41}$$

$$\mathcal{L}_{\text{uniform}}(f;t) \triangleq \log \mathop{\mathbb{E}}_{\substack{\text{i.i.d} \\ (\hat{h}_i, \hat{h}_j') \sim p_{\text{data}}}} \left[\exp(-t\|\hat{h}_i - \hat{h}_j'\|_2^2)\right], \quad t > 0 \tag{42}$$

And the second one is the $\mathcal{L}_{\text{dcl}}$ proposed by Yeh et al. (2021):

$$\mathcal{L}_{\text{dcl}} = -\log \frac{\exp\left(\hat{h}_i^T \hat{h}_i'/\tau\right)}{\sum_{j,j\neq i}^{N} \exp\left(\hat{h}_i^T h_j'\right)/\tau} = -\hat{h}_i^T \hat{h}_i'/\tau + \log \sum_{j,j\neq i}^{N} \exp\left(\hat{h}_i^T h_j'\right)/\tau \tag{43}$$

where the first term of equation 43 is acknowledged by DCL's authors to be equivalent to equation 41, while the difference between the second term and $\mathcal{L}_{\text{uniform}}$ is only the order of the logarithmic function and the first summation operation when the losses are calculated for all samples in the same mini-bacth. Their lower bounds can be obtained through Jensen's Inequality:

$$\begin{aligned} \mathcal{L}_{\text{uniform}} &= \log \frac{1}{M(N-1)} \sum_{i}^{M} \sum_{j,j\neq i}^{N} \left[\exp(-t\|\hat{h}_i - \hat{h}_j'\|_2^2)\right] \\ &\geq \frac{1}{M} \sum_{i}^{M} \log \frac{1}{N-1} \sum_{j,j\neq i}^{N} \left[\exp(-t\|\hat{h}_i - \hat{h}_j'\|_2^2)\right] \\ &\geq -\frac{t}{M(N-1)} \sum_{i}^{M} \sum_{j,j\neq i}^{N} \|\hat{h}_i - \hat{h}_j'\|_2^2 \end{aligned} \tag{44}$$

$$\mathcal{L}_{\text{dcl}}^{neg} = \log \sum_{j,j\neq i}^{N} \exp\left(\hat{h}_i^T h_j'\right)/\tau \tag{45}$$

$$
\begin{aligned}
\mathcal{L}_{\mathrm{dcl}}^{neg} - \log(N-1) =& \frac{1}{M}\sum_{i}^{M}\log\frac{1}{N-1}\sum_{j,j\neq i}^{N}\exp(\hat{h}_i^T h_j')/\tau \\
\geq& \frac{1}{\tau M(N-1)}\sum_{i}^{M}\sum_{j,j\neq i}^{N}\hat{h}_i^T h_j' \\
=& -\frac{1}{2\tau M(N-1)}\sum_{i}^{M}\sum_{j,j\neq i}^{N}\|\hat{h}_i - \hat{h}_j'\|_2^2 + \frac{1}{2\tau M(N-1)}
\end{aligned}
\tag{46}
$$

where M is batch size. Comparing equation 44 and 46, their common optimization objective is to maximize the sum of the squares of the Euclidean distance between all pairwise samples. Further, this optimization objective corresponds to a specific form of the minimum energy problem on the hypersphere Kuijlaars & Saff (1998); Liu et al. (2018), which is generalized from traditional Thomson Problem Thomson (1904) in physics.

E Relation with Mixup-based approaches

We focus on a class of Mixup-based methods Kalantidis et al. (2020); Zhang et al. (2022b) in contrastive learning which have similar optimization objectives to $\mathcal{L}_{\mathrm{mpt}}$. These methods that use Mixup Zhang et al. (2018) to generate hard negative samples for robustness and performance improvement, and they have been shown to be effective in VRL Kalantidis et al. (2020) and SRL Zhang et al. (2022b). It should to be noted that such methods are the improvements at the sample level, while do not change the property of "gradient dissipation" in contrastive loss.

Existing works generate mixup negative samples with two methods. The first one is generating by linearly weighting two hard negative sample representations Kalantidis et al. (2020). If we regard $\hat{h}_i$ as the anchor, the mixup negative sample can be defined as:

$$
\tilde{h}' = \frac{\lambda\hat{h}_m' + (1-\lambda)\hat{h}_n'}{\left\|\lambda\hat{h}_m' + (1-\lambda)\hat{h}_n'\right\|}, \quad m\neq i, n\neq i
\tag{47}
$$

where $\tilde{h}_j'$ represents the mixup hard negative sample and λ is the weight parameter. The second method is generating by linearly weighting the representations of a positive sample and a random negative sample Kalantidis et al. (2020); Zhang et al. (2022b):

$$
\tilde{h}' = \frac{\lambda\hat{h}_i' + (1-\lambda)\hat{h}_n'}{\left\|\lambda\hat{h}_i' + (1-\lambda)\hat{h}_n'\right\|}, \quad n\neq i
\tag{48}
$$

where λ should be less than 0.5 to avoid generating positive samples with high probability. Then we discuss the relation between both two generation methods with $\mathcal{L}_{\mathrm{mpt}}$. When M mixup negative samples are added to contrastive loss, the following inequality holds:

$$
\begin{aligned}
\mathcal{L}_{\mathrm{mix}} =& -\log\frac{\exp\left(\hat{h}_i^T\hat{h}_i'/\tau\right)}{\exp\left(\hat{h}_i^T\hat{h}_i'/\tau\right) + \sum_j^N\exp\left(\hat{h}_i^T\hat{h}_j'/\tau\right) + \sum_k^M\exp\left(\hat{h}_i^T\tilde{h}_k'/\tau\right)} \\
=& \log\left(1 + \frac{\sum_j^N\exp\left(\hat{h}_i^T\hat{h}_j'/\tau\right) + \sum_k^M\exp\left(\hat{h}_i^T\tilde{h}_k'/\tau\right)}{\exp\left(\hat{h}_i^T\hat{h}_i'/\tau\right)}\right) \\
=& \log\left(1 + \exp\left(-\hat{h}_i^T\hat{h}_i'/\tau\right)\left(\sum_j^N\exp\left(\hat{h}_i^T\hat{h}_j'/\tau\right) + \sum_k^M\exp\left(\hat{h}_i^T\tilde{h}_k'/\tau\right)\right)\right) \\
=& \log\left(1 + \exp\left(-\hat{h}_i^T\hat{h}_i'/\tau + \log\left(\sum_j^N\exp\left(\hat{h}_i^T\hat{h}_j'/\tau\right) + \sum_k^M\exp\left(\hat{h}_i^T\tilde{h}_k'/\tau\right)\right)\right)\right) \\
\leq& \log 2 + \max\left(-\hat{h}_i^T\hat{h}_i'/\tau + \log\left(\sum_j^N\exp\left(\hat{h}_i^T\hat{h}_j'/\tau\right) + \sum_k^M\exp\left(\hat{h}_i^T\tilde{h}_k'/\tau\right)\right), 0\right)
\end{aligned}
\tag{49}
$$

In the following we need to perform a secondary relaxation, and this process needs to be discussed on the following sub-conditions:

Condition 1 If $\tilde{h}'_k$ is generated using the way in equation 47, the maximum value of the N+M terms in the log function can be taken in the first N terms, and the following inequality holds:

$$\begin{aligned}
\mathcal{L}_{\text{mix}} &\leq \log 2 + \max\left(-\hat{h}_i^T \hat{h}'_i/\tau + \log\left(\sum_j^N \exp\left(\hat{h}_i^T \hat{h}'_j/\tau\right) + \sum_k^M \exp\left(\hat{h}_i^T \tilde{h}'_k/\tau\right)\right), 0\right) \\
&\leq \log 2 + \max\left(-\hat{h}_i^T \hat{h}'_i/\tau + \max_j\left(\hat{h}_i^T \hat{h}_j\right)/\tau + \log(N+M), 0\right) \\
&= \log 2 + \frac{1}{\tau}\max\left(-\hat{h}_i^T \hat{h}'_i + \max_j\left(\hat{h}_i^T \hat{h}_j\right) + \tau\log(N+M), 0\right)
\end{aligned} \tag{50}$$

Condition 2.1 If $\tilde{h}'_k$ is generated using the way in equation 48 and the maximum value of the N+M terms in the log function is taken in the first N terms, the inequality 50 still holds.

Condition 2.2 If $\tilde{h}'_k$ is generated using the way in equation 48 and the maximum value of the N+M terms in the log function is taken in the latter M term, the another inequality will hold:

$$\begin{aligned}
\mathcal{L}_{\text{mix}} &\leq \log 2 + \max\left(-\hat{h}_i^T \hat{h}'_i/\tau + \log\left(\sum_j^N \exp\left(\hat{h}_i^T \hat{h}'_j/\tau\right) + \sum_k^M \exp\left(\hat{h}_i^T \tilde{h}'_k/\tau\right)\right), 0\right) \\
&\leq \log 2 + \max\left(-\hat{h}_i^T \hat{h}'_i/\tau + \max_k\left(\hat{h}_i^T \tilde{h}_j\right)/\tau + \log(N+M), 0\right) \\
&= \log 2 + \max\left(-\hat{h}_i^T \hat{h}'_i/\tau + \max_k\left(\hat{h}_i^T \left(\lambda\hat{h}'_i + (1-\lambda)\hat{h}'_k\right)/\tau\right) + \log(N+M), 0\right) \\
&= \log 2 + \max\left(-\frac{1-\lambda}{\tau}\hat{h}_i^T \hat{h}'_i + \frac{1-\lambda}{\tau}\max_k\left(\hat{h}_i^T \hat{h}'_k\right) + \log(N+M), 0\right) \\
&= \log 2 + \frac{1-\lambda}{\tau}\max\left(-\hat{h}_i^T \hat{h}'_i + \max_k\left(\hat{h}_i^T \hat{h}'_k\right) + \frac{\tau}{1-\lambda}\log(N+M), 0\right)
\end{aligned} \tag{51}$$

This observation provides a novel perspective to explain the performance of $\mathcal{L}_{\text{mpt}}$: (1) if mixup negative samples are generated with the first method, the optimization objective of $\mathcal{L}_{\text{mpt}}$ will be equated to some extent with that of $\mathcal{L}_{\text{mix}}$ by appropriately adjusting m; (2) if mixup negative samples are generated with the second method, $\mathcal{L}_{\text{mix}}$ will have two different the upper bounds with different margins, $\tau\log(N+M)$ and $\frac{\tau}{1-\lambda}\log(N+M)$, during the training process. However, the margin m in $\mathcal{L}_{\text{mpt}}$ will no longer change during the optimization process.

Therefore, we establish the relation between the sample-level Mixup-based approaches and $\mathcal{L}_{\text{mpt}}$. By using a appropriate m, the optimization objective of $\mathcal{L}_{\text{mpt}}$ can be similar or equal to the mixup-based methods, which provides a new perspective to explain the well-performance of $\mathcal{L}_{\text{mpt}}$-like loss functions.